Journal of Medicinal Chemistry, 53(17), 6490-6505

Novel Carbamates as Orally Active Acetylcholinesterase Inhibitors Found to Improve Scopolamine-Induced Cognition Impairment: Pharmacophore-Based Virtual Screening, Synthesis and Pharmacology

*Shailendra S. Chaudhaery[1], Kuldeep K. Roy[1], Neeraj Shakya[1], Gunjan Saxena[2], Shreesh Raj Sammi[3], Aamir Nazir[3], Chandishwar Nath[3], Anil K. Saxena[1]**
[1]Division of Medicinal and Process Chemistry; [2]Division of Pharmacology; [3]Division of Toxicology, Central Drug Research Institute, CSIR, Lucknow (India)-226001

TITLE RUNNING HEAD: Novel Carbamates as Potent Acetylcholinesterase Inhibitors

CORRESPONDING AUTHOR FOOTNOTE:
* To whom correspondence should be addressed. Phone: (522) 2612412/ex4386. Fax: (522) 26123405. E-mail: anilsak@gmail.com.
[1]Division of Medicinal and Process Chemistry[2]Division of Pharmacology
[3]Division of Toxicology, Central Drug Research Institute, CSIR, Lucknow (India)-226001
CDRI communication number 7948

ABBREVIATIONS: AD, Alzheimer's disease; AChE, acetylcholinesterase; BChE, butyrylcholinesterase VS, virtual screening; NMDA, N-methyl-D-aspartate; CADD, computer-aided drug design; PBVS, pharmacophore-based VS; SBVS, structure-based VS; SAR, structure-activity relationship; QSAR, quantitative structure-activity relationship; MTDLs, multi-target directed ligands.

ABSTRACT

A systematic virtual screening (VS) experiment, consisting of the development of 3D-pharmacophore, screening of virtual library, synthesis and pharmacology, is reported. The predictive pharmacophore model (correlation = 0.955) with one H-bond donor and three hydrophobic features was developed using HypoGen on a training set of 24 carbamates as AChE inhibitors. The model was validated on a test set of 40 carbamates (correlation = 0.844). The pharmacophore-based VS of virtual library led to the identification of novel carbamates as potent AChE inhibitors. The synthesis and pharmacological evaluation of 9 carbamates against three diverse assay systems, namely (i) *in-vitro* Ellman method, (ii) *in-vivo* passive avoidance test and (iii) aldicarb-sensitivity assay, led to the discovery of orally active novel AChE inhibitors which improved Scopolamine-induce cognition impairment in Swiss male mice. Finally, two novel lead compounds **85** and **86** are selected as candidate molecules for further optimization.

KEYWORDS**:** Alzheimer's disease**,** Acetylcholinesterase inhibitor, Carbamates, Pharmacophore, Virtual screening, Memory.

INTRODUCTION

Alzheimer's disease (AD) is a progressive irremediable disorder of elderly patients, which is characterized by extensive central cholinergic neuronal loss, resulting in loss of cognitive functions.[1, 2] The cholinesterase (ChE) enzymes, namely acetylcholinesterase (AChE; EC 3.1.1.7) and butyrylcholinesterase (BChE; EC 3.1.1.8), which are found in the central nervous system (CNS), catalyze the hydrolysis of acetylcholine (ACh) at a rate of >10,000 molecules per second.[3] The AChE enzyme is one of promising drug-like targets, which has led to few palliative drugs presently used for the treatment of AD. These drugs include tacrine, galanthamine, donepezil, and rivastigmine as acetylcholinesterase inhibitors (AChEI), and memantine as a noncompetitive N-methyl-D-aspartate (NMDA) antagonist for moderate improvement in memory and cognitive function.[4-10] However, memantine has recently been reported to block the α_7 receptor in hippocampal neurons more effectively than NMDA receptors.[11, 12] However, these drugs result in only mild to moderate improvement in memory and cognitive function, but lack the ability to prevent or slow the progressive neuro-degeneration.[13-19] Hence, newer approaches *viz.* Multi-target directed ligands (MTDLs) and β-amyloid targeted therapies are under investigation.

Active Site of AChE: The active site of human AChE, located at the base of the ~20Å deep and narrow gorge, [20, 21] consists of two subsites: (i) an "esteratic" subsite containing the catalytic machinery, and (ii) an "anionic" subsite responsible for binding the quaternary trimethylammonium tail group of the acetylcholine. The essential catalytic functional unit of the human AChE is the catalytic triad characterized by three amino acid residues, namely Ser203, His447, and Glu334.[22] The acetyl head group of AChE, which is directly involved in making and breaking of bonds, is being held in place by another important functional unit in the esteratic subsite known as oxyanion hole, formed by the peptidic NH groups of three crucial residues namely, Gly121, Gly122, and Ala204.[22] Site-directed mutagenesis experiment indicates that the three amino acid residues, namely Trp86, Glu202 and Phe337, play important role in binding of the quaternary trimethylammonium tail group in the anionic subsite.[23]

Current Approaches: In the recent past, two aspects *viz.* the complex etiology of AD and the involvement of different but related dysfunctions in its progression, have gradually attracted interests in the development of novel multifunctional drugs for the treatment of AD.[24] The therapeutic potential of AChE inhibitors has been empowered by the recent evidences illustrating that, apart from their role in the cognition management, they might aid in the reduction in the rate of neurodegeneration in the AD affected persons. In fact, AChE has been reported to exert secondary non-cholinergic functions related to its peripheral anionic site[25-27] in cell adhesion[28, 29] and differentiation.[30] Several recent investigations also support its role in mediating the processing and deposition of β-amyloid (Aβ) peptides.[31-35] In the past few decades, drug discovery efforts have shifted towards the design of more potent and selective cholinesterase (ChE) inhibitors with lesser side effects. The interest in the discovery of novel potent AChE inhibitors is expected to continue in future, as current AChE inhibitors lack perfection.

In such scenario, direct- and indirect- computer-aided drug design (CADD) techniques are of utmost importance in terms of being time-saving and cost-effective techniques. One of the rationale starting point for the design of novel scaffolds is the development of a ligand-based predictive model to derive different structural features essential for receptor binding, using ligand-based molecular modeling tools, such as SYBYL/comparative molecular field analysis (CoMFA)[36] and comparative molecular similarity indices analysis (CoMSIA)[37]; Catalyst/HypoGen and HipHop[38]. In the recent past, we have published few systematic 3D-QSAR CoMFA and CoMSIA studies on carbamate-class of AChE inhibitors, in which important physicochemical requirements for the potential inhibition of AChE enzyme are

reported.[39, 40] However, the development of a 3D-pharmacophore and its correct use in the VS of the available databases seem to be more relevant and time-saving approach, which may lead into the identification of new chemotypes with potent AChE inhibitory activity for the treatment of AD.

Pharmacophore modeling is done using a collection of structurally diverse compounds, known to bind the same active site of a protein i.e. same mode of action. The HypoGen algorithm provides quantitative pharmacophore models based on a set of compounds with biological activities spread over 3-4 orders of magnitude or more broader activity range, whereas the HipHop algorithm provides qualitative pharmacophore models based on a small set of known active compounds.[41-43] Most of the pharmacophore modeling tools entertain functional features, such as hydrogen bond donors (HBD), hydrogen bond acceptors (HBA), hydrophobic groups (HY), aromatic rings (AR), positively charged/ionizable groups (PG), and negatively charged/ionizable groups (NG). Additionally, shape and excluded volumes can be included into the pharmacophore models to represent the framework of the active site. Pharmacophore based virtual screening methods surpass structure based methods by their ability to screen very large databases faster and by their tendency to retrieve more structurally diverse leads.

In the present paper, we describe the development of quantitative pharmacophore model using a congeneric carbamate class of AChE inhibitors and its successful application in the virtual screening process. This has led to the identification of novel AChE inhibitors which are synthesized and evaluated for their AChE inhibition potential in *in-vitro* as well as *in-vivo* assay systems. Apart from the widely used assay systems, such as Ellman methods and Passive avoidance test, synthesized compounds have also been tested in a model system of *Caenorhabditis elegans*, which is a powerful *in-vivo* model for carrying out studies on neurochemical aspects of the organismal biology.[44] The *C. elegans* model holds relevance because of its appreciable homology of gene sequences and conservation of many disease pathways with humans, and most importantly for our studies is the presence of most of mammalian gene families involved in neuronal function in *C. elegans*.[44] Hence, employing this model system we have assessed, whether or not, our test compounds affect the release of neurotransmitter ACh in the synaptic cleft. The assay employs Aldicarb (an AChE inhibitor acts in the peripheral nervous system) to induce paralysis in the exposed *C. elegans* nematodes.[45] It is well known that the AChE enzyme is present in the synaptic cleft, which catalyzes the hydrolysis of neurotransmitter ACh to choline and acetate, and thus, eliminating ACh from synapse. The presence of aldicarb leads to the inhibition of AChE, which in turn results in the accumulation of ACh at the synaptic cleft. Such high level of ACh in the synaptic cleft causes over-activation of cholinergic receptors, hyper-contraction of muscles, and ultimately paralysis.[46] However, if any chemical or any mutation affects the ACh-AChE pathway in the nematodes, that would result in their altered response to aldicarb induced paralysis;[47] compounds increasing ACh release at the synaptic cleft would render the worms sensitive and compounds decreasing the release of ACh would lead to resistance of worms against aldicarb induced paralysis. This widely used assay system helped us in testing our predictive analysis.

RESULTS AND DISCUSSION

Pharmacophore Modeling: Among the generated pharmacophore models, based on the training set of 24 compounds (Figure 1), the results of the top 10 pharmacophore models are summarized in Table 1.

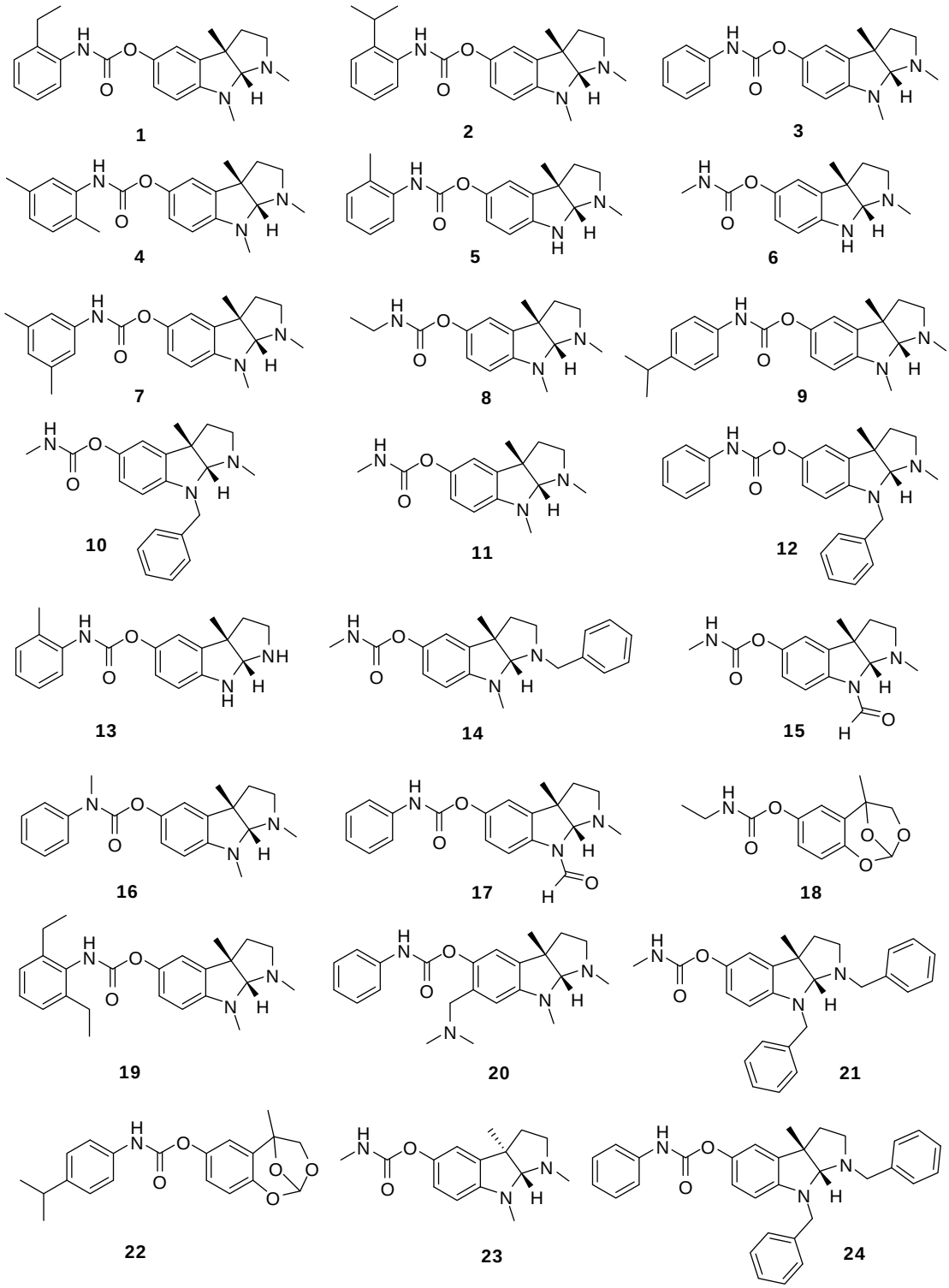

Figure 1: Chemical structures of the training set compounds.

Table 1: Summary of top 10 pharmacophore models obtained from Catalyst/HypoGen run.

Hypothesis	Features[a]	Total cost	Δ Cost[b]	rms[c]	Correl (r)
Hypo-01	HBD, HY, HY, HY	101.226	22.716	0.568	0.95
Hypo-02	HBA, HBD, HY, HY, HY	106.122	17.820	0.827	0.90
Hypo-03	HBA, HBD, HY, HY, HY	111.625	12.317	1.115	0.80

Hypo-04	HBA, HBD, HY, HY, HY	113.413	10.520	1.153	0.79
Hypo-05	HBD, HY, HY, HY, HY	113.850	10.092	1.208	0.77
Hypo-06	HBA, HBD, HY, HY, HY	114.988	8.950	1.240	0.75
Hypo-07	HBA, HBA, HY, HY, HY	116.334	7.600	1.260	0.74
Hypo-08	HBA, HBD, HY, HY, HY	119.520	4.422	1.370	0.69
Hypo-09	HBA, HBD, HY, HY, HY	119.855	4.092	1.250	0.75
Hypo-10	HBA ,HBD, HY, HY	120.314	3.628	1.400	0.67

[a] HBD = hydrogen bond donor, HBA = hydrogen bond acceptor, HY = hydrophobic features; [b] cost difference between total cost of the corresponding hypothesis and the cost of the null hypothesis (123.942); [c] root mean square deviation (Note: Fixed cost of the hypothesis was 96.305)

The total cost of each pharmacophore model was close to the fixed cost value, which is expected for a good pharmacophore model, and hence, for an efficient HypoGen run. The term 'cost' in HypoGen algorithm indicates the number of binary bits required to generate a particular pharmacophore/hypothesis. The HypoGen algorithm performs three important theoretical cost calculations, namely fixed, null and total costs, as determinants of the superiority of any particular pharmacophore model over others. The configuration cost was also within the allowed range (≤ 17.000). The difference between the null cost (123.942) and the fixed cost (96.305) was 27.637, while the difference between the null cost and the total cost (101.226) of the best pharmacophore model (Hypo-01; Figure 2) was 22.716 bits. The probable explanations for observed lower value of the cost difference (residual cost) in the present study as well as previously reported in the literature[48, 49] may be due to the presence of fairly rigid and structurally homologous molecules in the training set. The best pharmacophore model (Figure 2), comprising three hydrophobic (HY) and one hydrogen bond donor (HBD) features along with 34 excluded volumes, was found to be the most significant in terms of its high correlation (r) of 0.955 and low root mean square (rms) error of 0.569 only. A very small difference (only 5 bits) between the total and fixed costs additionally demonstrated the significance of the best pharmacophore model. The observed and estimated AChE inhibitory activities of the training set compounds, by Hypo-01, is given in Table 2, while the graph between the two is given in Figure 3.

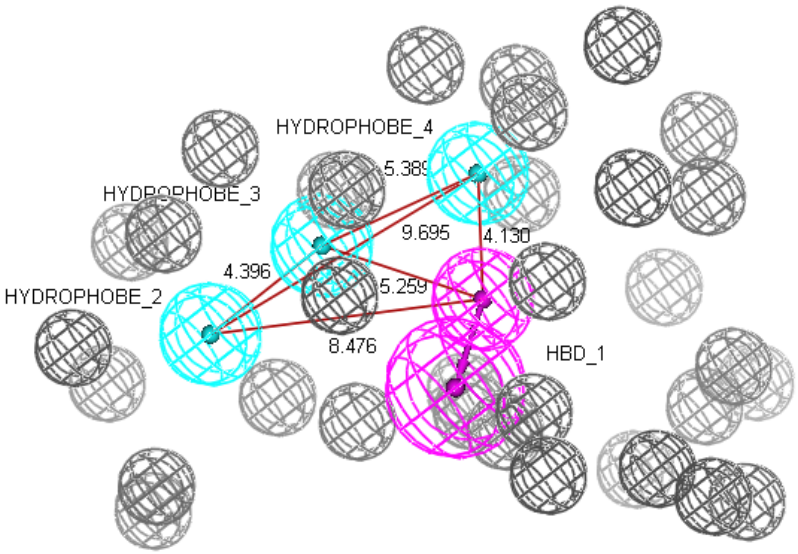

Figure 2: The best pharmacophore model comprising three hydrophobic, one hydrogen bond donor and a set of 34 excluded volumes.

Table 2: Observed and estimated AChE inhibitory activities (IC_{50}, nM) of the training set molecules by the best pharmacophore model (Hypo-01).

Comp	FitValue	IC_{50} (nM)		Activity Scale[c]		pIC_{50} (Est.; nM)	pIC_{50} (Obs.; nM)
		Est.[a]	Obs.[b]	Est.	Obs.		
1	5.64	5.00	10.00	+++	+++	-0.699	-1.000
2	4.90	27.00	15.00	+++	+++	-1.431	-1.176
3	4.52	66.00	22.10	+++	+++	-1.820	-1.344
4	4.92	26.00	26.00	+++	+++	-1.415	-1.415
5	4.88	29.00	40.00	+++	+++	-1.462	-1.602
6	4.52	65.00	56.70	+++	+++	-1.813	-1.754
7	4.28	120.00	78.00	++	+++	-2.079	-1.892
8	4.29	110.00	94.00	++	+++	-2.041	-1.973
9	4.55	61.00	110.00	+++	++	-1.785	-2.041
10	4.28	110.00	160.80	++	++	-2.041	-2.206
11	4.23	130.00	210.00	++	++	-2.114	-2.322
12	3.62	520.00	245.30	+	++	-2.716	-2.390
18	2.97	2300.00	830.00	+	+	-3.362	-2.919
19	3.53	640.00	1500.00	+	+	-2.806	-3.176
20	2.94	2500.00	2500.00	+	+	-3.398	-3.398
13	3.62	520.00	285.00	+	++	-2.716	-2.455
14	3.79	350.00	330.00	++	++	-2.544	-2.519
15	3.89	280.00	387.50	++	++	-2.447	-2.588
16	3.95	240.00	690.00	++	+	-2.380	-2.839
17	3.07	1800.00	780.40	+	+	-3.255	-2.892
21	3.05	2000.00	3560.00	+	+	-3.301	-3.551
22	2.59	5500.00	4300.00	+	+	-3.740	-3.633
23	2.81	3400.00	9887.00	+	+	-3.531	-3.995
24	1.55	61000.00	41130.00	+	+	-4.785	-4.614

[a] Est. = estimated; [b] Obs. = observed; [c] Activity scale: +++ (IC_{50} < 100nM, highly active), ++ (100 < IC_{50} < 500 nM, moderately active), + (IC_{50} > 500 nM, poorly active).

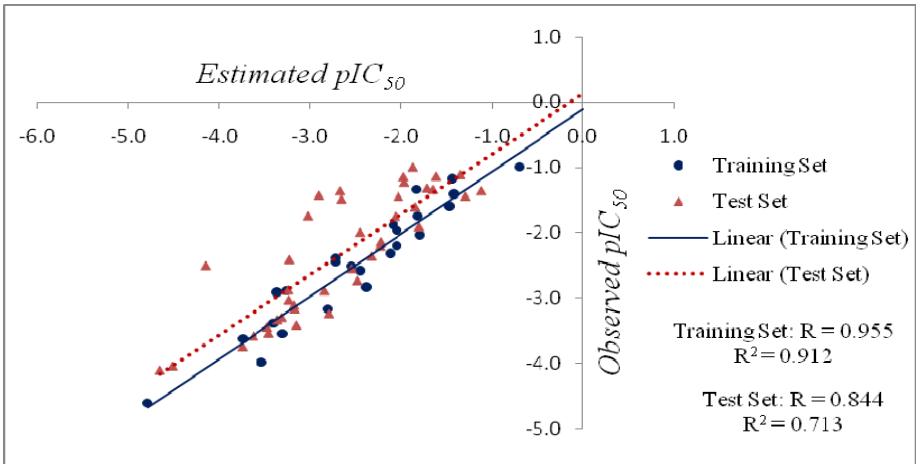

Figure 3: 2D scatter plot between observed and estimated AChE inhibitory activities (pIC_{50}) of the training (blue coloured dots) and test set (magenta coloured triangles) compounds.

The training set compounds were estimated very accurately by the best pharmacophore model with considerably low rms error, and were correctly categorized into highly active, moderate active and inactive classes, with few exceptions *e.g.* the two active compounds, namely **7** and **8,** were estimated to be moderate active, and the two moderate active compounds, namely **12** and **13,** were estimated to be inactive (Table 2).

Model Validation: Apart from the internal statistics such as correlation, cost-function quality and ability to explain the training set compounds, an additional validation of the model using the test set (referred as test set validation) is one of the mandatory steps for establishing its competency for prediction accuracy as well as classification quality among the test set compounds, which were kept aside during the model development process. Therefore, in the present study, the best pharmacophore model was further validated using the test set of 40 compounds (Table 3). As expected, the best pharmacophore model well performed in this crucial step and well explained the AChEI activity variation among the test set compounds with correlation (r) of 0.844 (r^2 = 0.713; Figure 3). This further substantiated its significance, and thereby provided an added assurance of its suitability for the use in the virtual screening process to identify novel potent AChE inhibitors. The observed and estimated AChE inhibitory activities of the test set compounds is given in the supporting information.

Table 3: Details of the 40 compounds in the test set

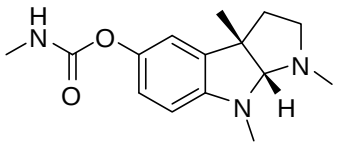

25

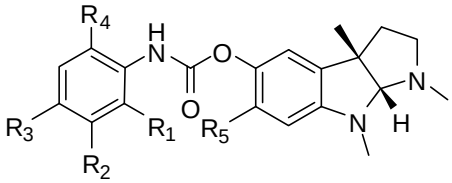

26 - 35

Comp	R_1	R_2	R_3	R_4	R_5	AChEI Activity (pIC_{50}; nM)		Activity Scale	
						Obs.	Est.	Obs.	Est.
25	…	…	…	…	…	-1.45	-1.30	+++	+++
26	H	H	H	H	H	-1.34	-1.65	+++	+++
27	Methyl	H	H	H	H	-1.00	-1.87	+++	+++
28	H	H	Methyl	H	H	-2.15	-3.23	++	++
29	Methyl	H	Methyl	H	H	-1.15	-1.97	+++	+++
30	Methyl	CH3	H	H	H	-1.36	-2.67	+++	++
31	H	CH3	Methyl	H	H	-1.49	-2.66	+++	++
32	Methyl	H	H	Methyl	H	-2.89	-2.84	+	+
33	H	H	H	H	Methyl	-2.41	-3.22	++	+
34	Methyl	H	Methyl	Methyl	H	-3.11	-3.17	+	+
35	H	H	Isopropyl	H	H	-2.88	-3.24	+	+

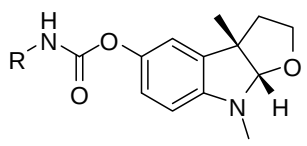

36-39

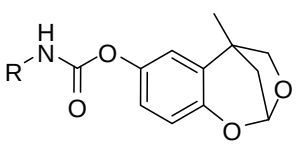

40 & 41

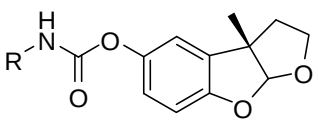

42 & 43

Comp	R	AChEI Activity (pIC_{50}; nM)	Activity Scale

		Obs.	Est.	Obs.	Est.
36	Methyl	-1.43	-2.90	+++	+
37	Ethyl	-1.91	-1.80	+++	+++
38	(2-methyl)phenyl	-1.11	-1.35	+++	+++
39	(4-isopropyl)phenyl	-3.59	-3.62	+	+
40	Ethyl	-2.56	-2.55	++	++
41	(2-methyl)phenyl	-1.75	-3.02	+++	+
42	(2-methyl)phenyl	-1.36	-1.12	+++	+++
43	(4-isopropyl)phenyl	-3.42	-3.15	+	+

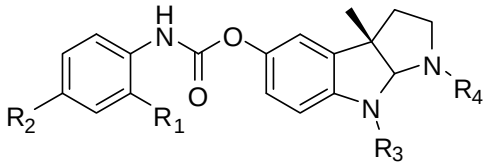

44-50

Comp	R_1	R_2	R_3	R_4	AChEI Activity (pIC_{50} (nM)		Activity Scale	
					Obs.	Est.	Obs.	Est.
44	H	Isopropyl	Methyl	H	-2.51	-4.15	++	+
45	Methyl	H	Methyl	H	-1.23	-1.96	+++	+++
46	Methyl	H	Methyl	Phenethyl	-2.74	-2.48	+	++
47	H	Isopropyl	Benzyl	Methyl	-4.11	-4.65	+	+
48	H	Isopropyl	H	Methyl	-3.31	-3.31	+	+
49	Methyl	H	Benzyl	Methyl	-2.00	-2.45	++	++
50	Methyl	H	Benzyl	Benzyl	-3.25	-2.79	+	+

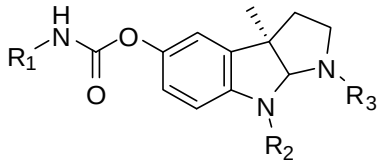

51-59

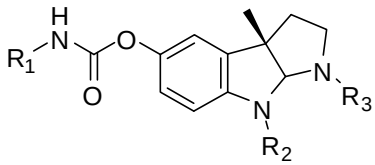

60-64

Comp	R_1	R_2	R_3	AChEI Activity (pIC_{50} (nM)		Activity Scale	
				Obs.	Est.	Obs.	Est.
51	Methyl	Benzyl	Methyl	-3.45	-3.47	+	+
52	Phenyl	Benzyl	Methyl	-4.05	-4.51	+	+
53	Methyl	H	Methyl	-3.34	-3.36	+	+
54	Phenyl	H	Methyl	-3.75	-3.74	+	+
55	Phenyl	Methyl	Methyl	-3.54	-3.45	+	+
56	Phenyl	Methyl	H	-1.14	-1.62	+++	+++
57	Methyl	Methyl	H	-1.32	-1.71	+++	+++
58	Methyl	H	Methyl	-1.75	-2.06	+++	++
59	Phenyl	H	H	-2.36	-2.33	++	++
60	Phenyl	H	Methyl	-1.61	-1.84	+++	+++
61	Methyl	Methyl	Methyl	-1.45	-2.03	+++	++
62	Methyl	H	H	-3.17	-3.17	+	+

63	Methyl	Benzyl	Benzyl	-3.04	-3.23	+	+
64	Methyl	Benzyl	Methyl	-2.21	-2.23	++	++

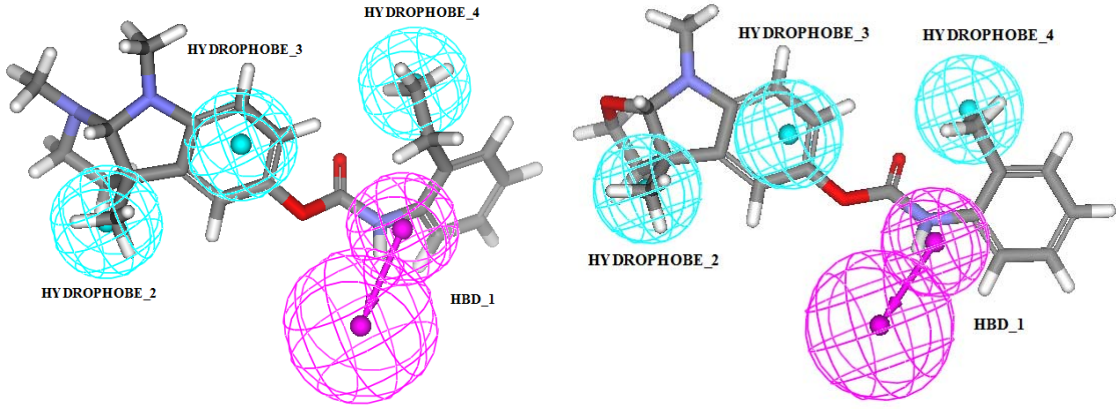

1 **38**

Figure 4: Pharmacophore mapping of the most active compounds *viz.* **1** (left) and **38** (right) in the training and test set respectively.

The Hypo-01 was further studied for its mapping pattern, and thereby classification among the highly active, moderately active and inactive (or lesser active) compounds in the training and test set. The mapping analysis of the highly active compounds, namely **1** and **38** in the training and test set respectively, revealed that none of the essential pharmacophoric features were missed and all features mapped with the least displacement from the centroid of all features (Figure 4). The angular methyl group of compounds, namely **1** and **38**, mapped well with the HYDROPHOBE_2 feature of the Hypo_01, while phenyl ring of the non-carbamate core of each molecule mapped with the HYDROPHOBE_3. The carbamoyl NH mapped to the HBD_1 feature, while the HYDROPHOBE_4 feature mapped to the ethyl and methyl groups of compounds **1** and **38** respectively. The moderate and lesser active (inactive) compounds missed to map one or more pharmacophoric features, and thereby well recommended their corresponding categories.

Complementarity between Best Pharmacophore and Active Site Residues of AChE: One of the most remarkable features of the AChE enzyme is the high aromatic content of ~20Å deep and cylindrical active-site gorge, which is lined by 14 conserved aromatic amino acids, namely Phe120, Phe288, Phe290, Phe330, Phe331, Trp84, Trp233, Trp279, Trp432, Tyr70, Tyr121, Tyr130, Tyr334, and Tyr442.[50] The X-ray crystallographic studies have also established the involvement of several of these conserved aromatic residues in interactions with AChE inhibitors *via* both π-cation and π–π stacking interactions.[50] Therefore, it appears that the hydrophobic interaction between the AChE enzyme and its inhibitors is one of the most salient features present, which was also reported by us previously based on 3D-QSAR comparative molecular field analysis (CoMFA) and comparative molecular similarity indices analysis (CoMSIA) studies.[39, 40] Among the known co-crystallized structures of *Torpedo californica* AChE available in the RCSB Protein Data Bank (www.rcsb.org), one is co-crystallized with Rivastigmine (PDB-Id: 1GQR[51]), and other one is with Ganstigmine (PDB-Id: 2BAG[52]). Among these two co-crystallized AChE inhibitors, Rivastigmine is present in the broken form (Figure 5) with carbamate part being covalently bound with Ser200 while rest non-carbamate part remains in the anionic subsite lined by Trp84 and Phe330 residues of the catalytic site (CAS). In case of 2BAG, the carbamate part is covalently bound with the

Ser200 but the non-carbamate part is absent. Docking of the most active compound **1** into the active site of AChE enzyme, using the GOLD[53] program, revealed that all mapped pharmacophoric features of the best pharmacophore (Hypo-01) well complemented with the active site residues (Figure 5), which further substantiated the acceptability of the best pharmacophore. The two residues, namely Trp84 and Phe330 of the anionic subsite correspond to HYDROPHOBE_2 and HYDROPHOBE_3 respectively, while the projection of carbamoyl amino group towards His440 corresponds to HBD_1 feature, and the hydrophobic group attached to the carbamoyl nitrogen resides in the acyl pocket surrounded by Trp233, Phe288 and Phe290 residues and corresponds to the HYDROPHOBE_4 feature of the best pharmacophore.

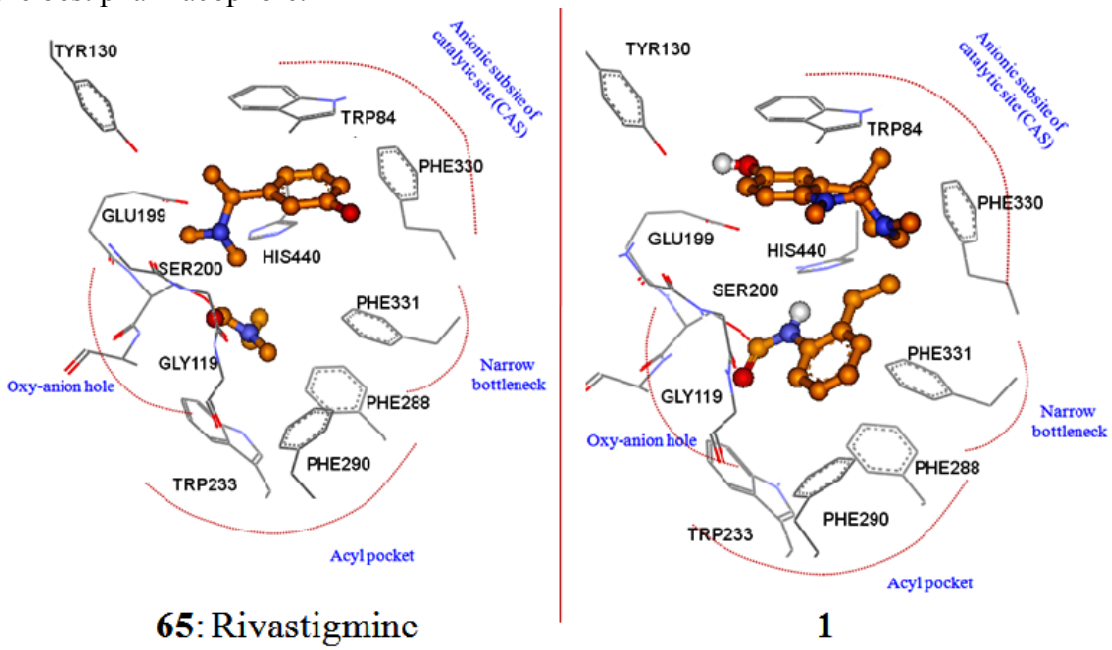

Figure 5: Stereo-view of binding poses of broken carbamate and non-carbamate fragments of the compound **65** (Rivastigmine) and **1** in the active site of AChE enzyme. Fragments are displayed in the orange coloured ball and stick form while the active site residues are displayed as lines.

Apart from the test set validation, a set of 13 known potent AChE inhibitors[54-62] (Figure 6) were collected from the literature for external validation of the best pharmacophore (Hypo-01). This model well mapped and predicted the AChEI activity of these additional compounds, and further added to the robustness of the model. The estimated and observed AChEI activities of these compounds are given in Table 4, while their pharmacophore mapping patterns are given in the supporting information.

Table 4: Observed and estimated AChEI activities (IC_{50}, nM) of 13 compounds of the external set by the best pharmacophore model (Hypo-01)

Name	FitValue	IC_{50} (nM)		Reference
		Est.[a]	Obs.[b]	
65 (Rivastigmine)	3.061	1900.53	4150.00	72
66 (Physostigmine)	4.520	65.00	56.70	72
67 (Eptastigmine)	4.704	43.228	22.00	72
68 (Phenserine)	4.518	66.00	22.10	72
69 (Tolserine)	4.88	29.00	40.00	72

70	4.526	65.196	32.00	61
71 (CHF2819)	4.567	59.316	125.00	72
72 (Quilostigmine; NXX-066)	4.232	128.361	148.00	57
73 (P10358)	4.449	77.842	100.00	60
74	4.396	87.86	8.11	58
75	4.126	163.87	30.00	58
76	4.556	60.784	17.30	58
77	4.360	95.435	7.00	62

[a] Est. = estimated; [b] Obs. = observed

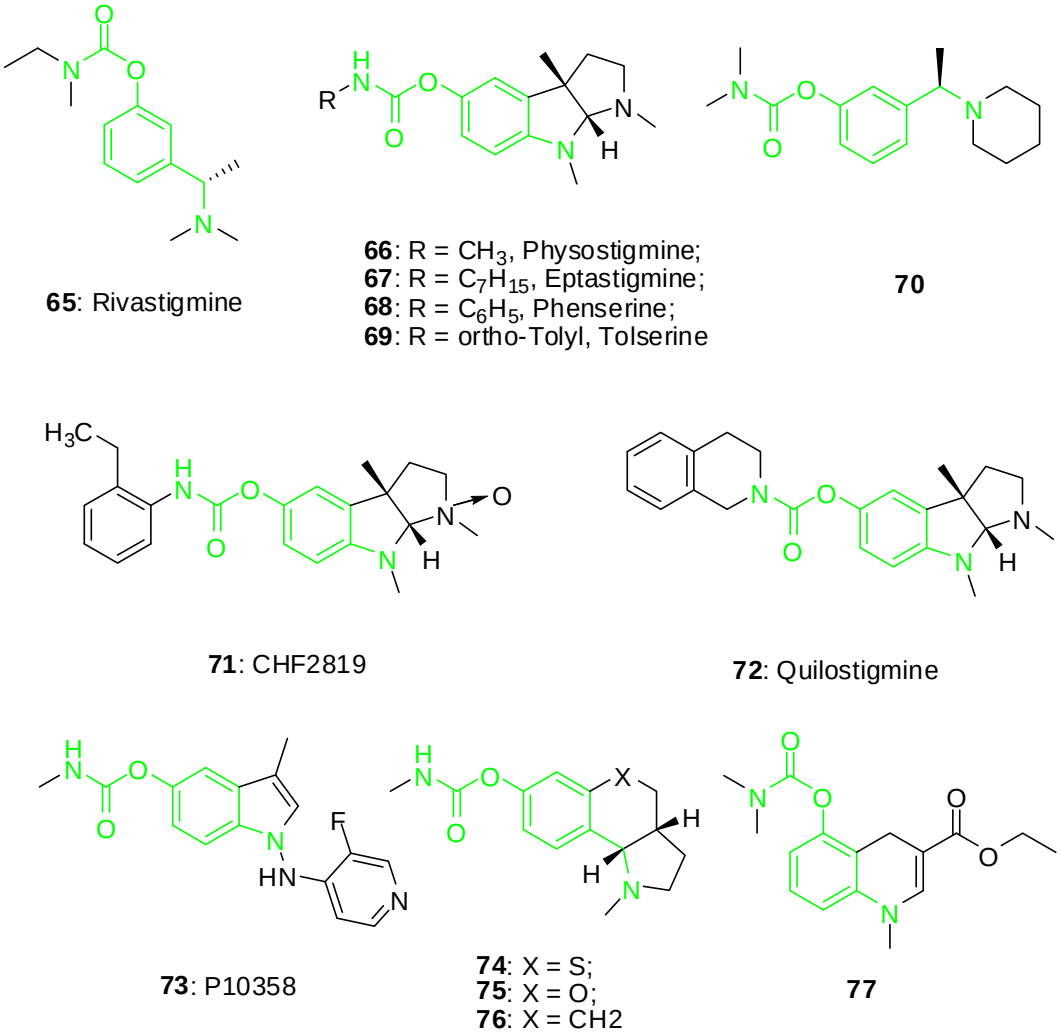

Figure 6: Carbamates reported as AChE inhibitors (Note: Green coloured part in each structure indicates common substructure/core).

Core Hopping and Virtual Library Generation:

Core Hopping refers to the process of searching of novel core, which matches with the known core in the reported highly active inhibitors/drugs for the particular activity. In the present study, we applied our state-of-art in the design of the core using a very well applied approach known as substructure searching. However, in the substructure (core) searching approach, the most crucial task is the selection of the substructure (core). In our opinion, the best way to gain an insight into the possible substructure (core) should be based on the structures of the reported clinically effective inhibitors/drugs, which has either reached into the market of had succeeded in the clinical trial phases.

Common core analysis (green coloured parts in Figure 6) among the known clinically effective carbamate class of AChE inhibitors[54-62] led us to proceed with the 4-carbamoylphenylmethylamine core (Figure 7) in the design of the novel core and its use in the generation of virtual combinatorial library. The strategy adopted for the novel core design is outlined in Figure 7.

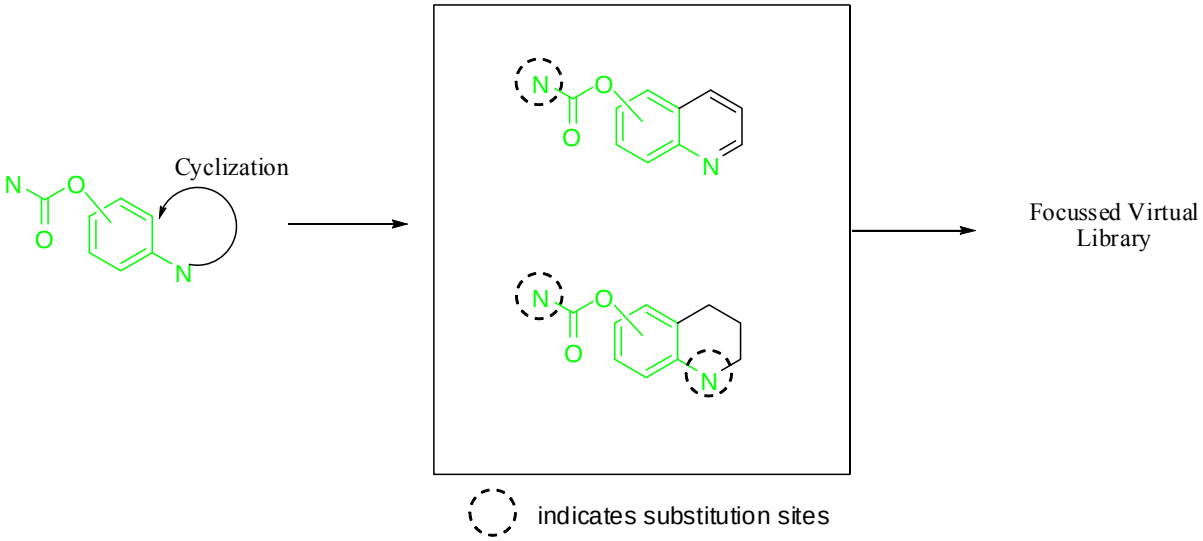

Figure 7: Strategies adopted during core hopping and virtual library generation.

The virtual combinatorial library was generated using CombiGlide module[63] implemented in the Schrodinger software[64] in which substituted/ unsubstituted alkyl, aryl, heteroaryl and other groups at the substitution sites (circled in Figure 7) in the designed cores. The generated virtual library was subjected to the Build Database protocol implemented in the Accelry's DS2.0, which provided a multi-conformer database for the use in the pharmacophore-based virtual screening (PBVS) protocol.

Pharmacophore-Based Virtual Screening: The PBVS has been a well adopted *in-silico* high-throughput screening process for identification and optimization of novel lead molecules. In search of potent AChE inhibitors, the best pharmacophore model (Hypo-01) was used in the PBVS protocol using the multi-conformer database, which in turn led to the identification of novel carbamates as potent AChE inhibitors. Among the identified molecules, a set of 9 prioritized compounds **85-93** (Table 5) were targeted for synthesis and pharmacological evaluation to test the best hypothesis (Hypo-01). Figure 8 shows the overlay of two most active compounds (**92** and **93**) over the best pharmacophore. These two compounds mapped all features very well with n-heptyl and chloro groups of compound **92** and **93** respectively mapped to the HYDROPHOBE_4, while their carbamoyl NH mapped to HBD_1. Other two features *viz.* HYDROPHOBE_2 and HYDROPHOBE_3 mapped to the pyridyl and phenyl rings of the quinoline respectively with slightly higher displacement from their centroids. Figure 9 shows the docked poses of the carbamate and non-carbamate fragments of compounds **86** and **93**, where it is clear that the two residues, namely Trp84 and Phe330 of the anionic subsite correspond to HYDROPHOBE_2 and HYDROPHOBE_3 respectively, while the projection of carbamoyl amino group towards His440 corresponds to HBD_1 feature, and the hydrophobic group attached to the carbamoyl nitrogen resides in the acyl pocket surrounded by Trp233, Phe288 and Phe290 residues and corresponds to the HYDROPHOBE_4 feature of the best pharmacophore.

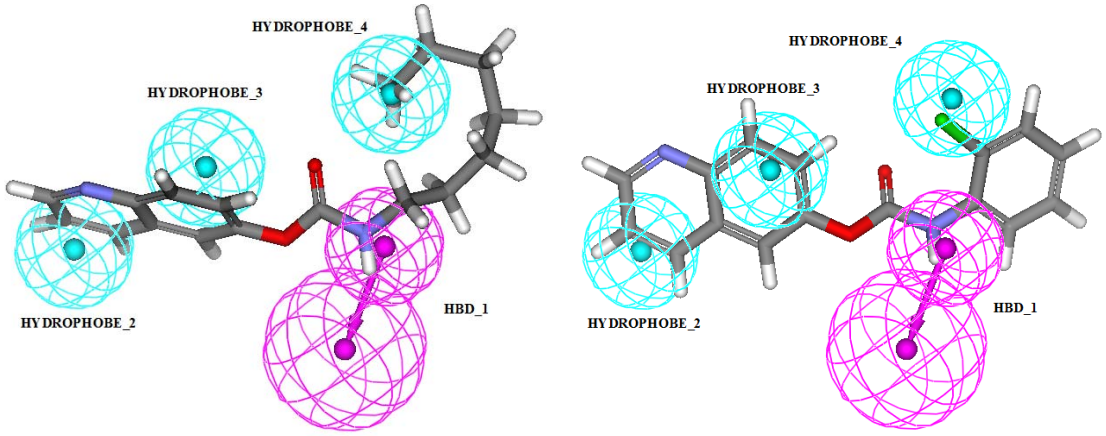

Figure 8: Pharmacophore mapping of the two most active compounds.

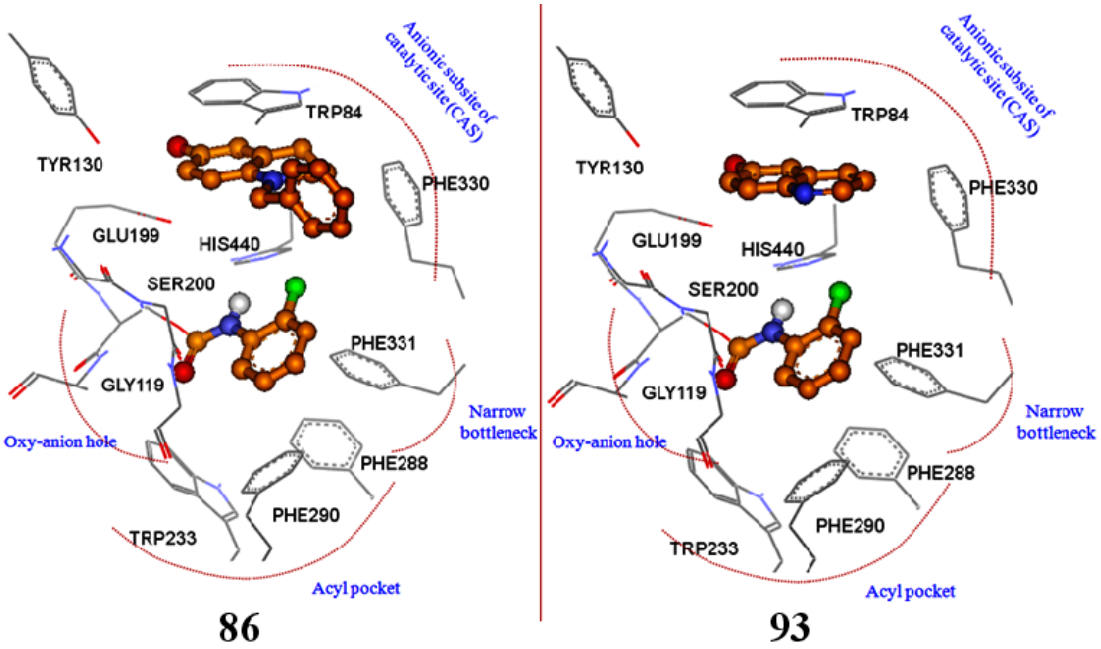

Figure 9: Stereo-view of binding poses of broken carbamate and non-carbamate fragments of the compound **86** and **93** in the active site of AChE enzyme. Fragments are displayed in theorange coloured ball and stick form while the active site residues are displayed as lines

Table 5: Chemical Structures of designed compounds and their AChE inhibitory (*in-silico* & *in-vitro*) and *in-vivo* learning improvement activities.

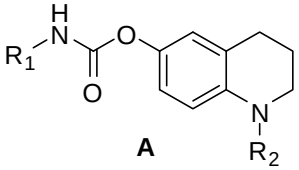

A

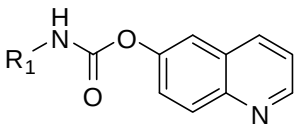

B

Compd.	Type	R_1	R_2	AChEI Activity (IC_{50}; nM)		Passive Avoidance Test		
						Trials		% LI$^{\neq}$
				Estimated	Observed	1st	2nd	
85	A	n-Hexyl	Bn	87.36	ND**	92.00	205.00	89.190
86	A	2-Chlorophenyl	Bn	141.22	3310	83.50	186.40	89.597

87	A	3-Bromophenyl	H	313.92	ND	97.00	195.00	67.395
88	A	4-Chloro-3-trifluoromethylphenyl	H	411.03	ND	133.00	222.20	33.431
89	A	4-Bromophenyl	H	233.88	ND	120.00	216.40	46.697
90	A	4-Chloro-3-trifluoromethylphenyl	Me	134.16	ND	104.00	218.00	75.979
91	A	4-Bromophenyl	Me	328.43	ND	124.00	242.00	61.525
92	B	n-Heptyl	--	99.83	ND	99.00	238.00	106.768
93	B	2-Chlorophenyl	--	86.50	ND	89.60	230.00	123.060
		Scopolamine*		--	--	110.00	147.00	0
		Donepezil		--	90.00	91.40	245.00	134.416
		Tacrine		--	800	73.40	241.00	194.702

*(3 mg/kg, ip), ** ND = not determined due to coloured nature of compound and/or solubility problem, $^{\neq}$% learning improvement: % learning in treated group - % learning in Scopolamine group, where % learning: 2nd trial - 1st trial/1st trial] x 100.

Chemistry: The synthesis of the intermediates (**78-84**) and designed compounds (**85-93**) is outlined in Scheme 1. The 6-methoxyquinoline (**78**) was partially reduced to 6-methoxy-1, 2, 3, 4-tetrahydroquinoline (**79**) using Nickel-aluminium alloy, ethanol and 10% NaOH in water (w/v) at ambient temperature. The N-benzylation of 6-methoxy-1, 2, 3, 4-tetrahydroquinoline (**79**) was done using benzyl chloride in the presence of potassium carbonate (K_2CO_3) and potassium iodide (KI) as inorganic bases in anhydrous N, N-dimethylformamide (DMF) as the organic solvent. The N-methylation of 6-methoxy-1, 2, 3, 4-tetrahydroquinoline (**79**) was done using methyl iodide in the presence of sodium hydride (NaH) as an inorganic base in anhydrous DMF at -10 to 30ºC. The conversion of 6-methoxyquinoline (**79**), N-benzyl-6-methoxy-1,2,3,4-tetrahydroquinoline (**80**) and N-methyl-6-methoxy-1,2,3,4-tetrahydroquinoline (**81**) into respective 6-hydroxyquinoline (**82**), N-benzyl-6-hydroxy-1,2,3,4-tetrahydroquinoline (**83**) and N-methyl-6-hydroxy-1,2,3,4-tetrahydroquinoline (**84**) was accomplished by refluxing corresponding methoxy intermediates in 47% HBr in water (v/v) solution for 5-8 hours. The reaction of corresponding hydroxyl intermediates namely, **82**, **83**, **84** with substituted or unsubstituted alkyl/aryl isocyanates using dry tetrahydrofuran (THF) as solvent in the presence of one of the inorganic bases like NaH, pyridine *etc* yielded corresponding carbamate derivatives namely **85**, **86**, **90**, **91**, **92**, **93** *etc* as final desired compounds. The N-debenzylation was accomplished using 10% Pd-C catalyst and H_2 at 50 psi to afford title compounds **87-89**.

Scheme 1:

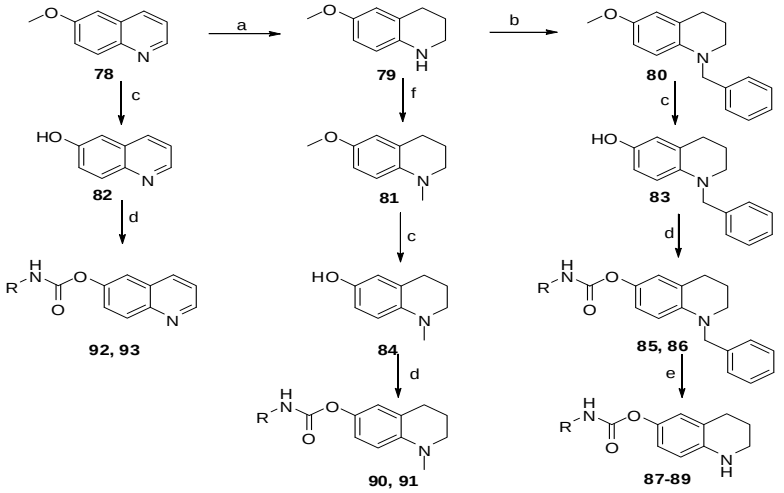

Reagents and conditions: a. Nickel-aluminium alloy, ethanol, 10% NaOH in water (w/v), 5-6 hrs; **b**. benzyl chloride, dry DMF, baked K_2CO_3 (or $NaCO_3$), NaI (or KI), 80°C, 3-5 hr; **c**. 47% HBr in water (v/v), reflux, 5-8 hrs; **d**. RNCO, NaH, THF; **e**. 10% Pd-C, MeOH, H_2 at 50 psi; **f**. CH_3I, NaH, DMF, -10 to 30°C

Pharmacological Results: All compounds were evaluated using three diverse assay systems: (i) *in-vitro* assay method described by Ellman *et al.*[65] (ii) *in-vivo* passive avoidance test[66] conducted in adult Swiss male mice of 3-4 months (wt. 20-25 g) and (iii) *in-vivo* assay called aldicard-sensitivity assay employing *C. elegans* as model system.[44, 46] Scopolamine induced impairment in passive avoidance test (*in-vivo*) and the inhibition of AChE in rodents are commonly employed screening tests to predict the potential of an AChE inhibitor as cognitive enhancer (anti-dementic) drug.[67] Table 5 summarizes the *in-silico* estimated and *in-vitro* observed AChE inhibitory (AChEI) activities, and also the *in-vivo* activity data (% LI; Passive avoidance test) of the synthesized compounds (**85-93**), and Tacrine and Donepezil as reference compounds. Figure 10 describes the transfer latency time (TLT; sec) in the first and second trial of the synthesized compounds (**85-93**), and Donepezil. Figure 11 shows the *in-vivo* data obtained from the biological assay employing *C. elegans* model system (aldicard-sensitivity assay). The results of compounds, namely Donepezil, **85**, **86**, **89** and **93** were significant at $p < 0.05$, whereas the compound **88** was significant at $p < 0.001$ in the aldicarb-sensitivity assay.

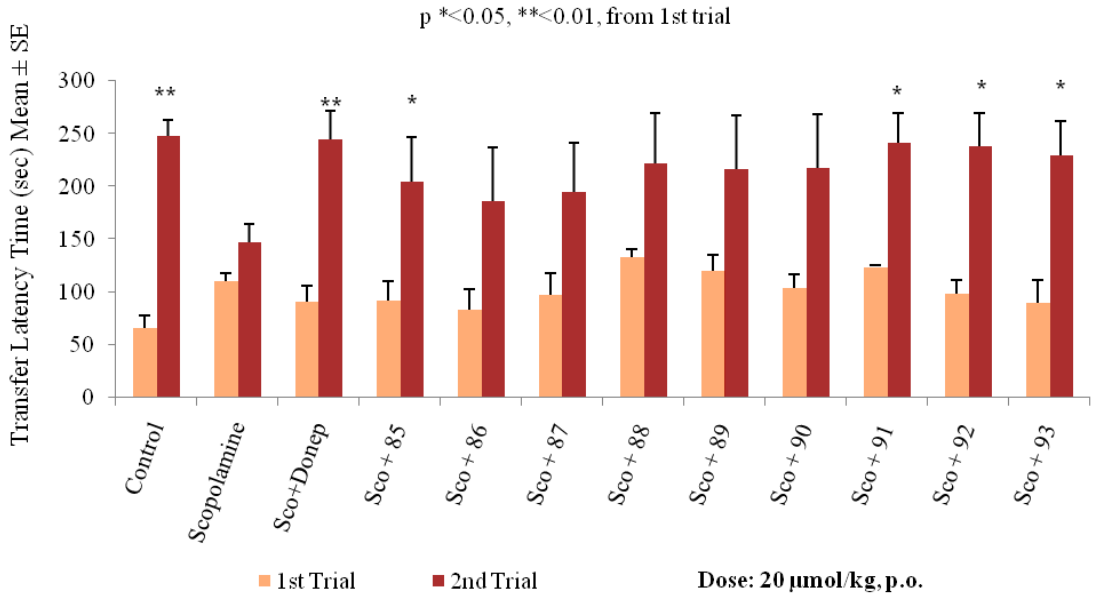

Figure 10: *In-vivo* results of Scopolamine induced deficit (dementia/amnesia) in adult Swiss male mice (Passive Avoidance Test) of the screened compounds.

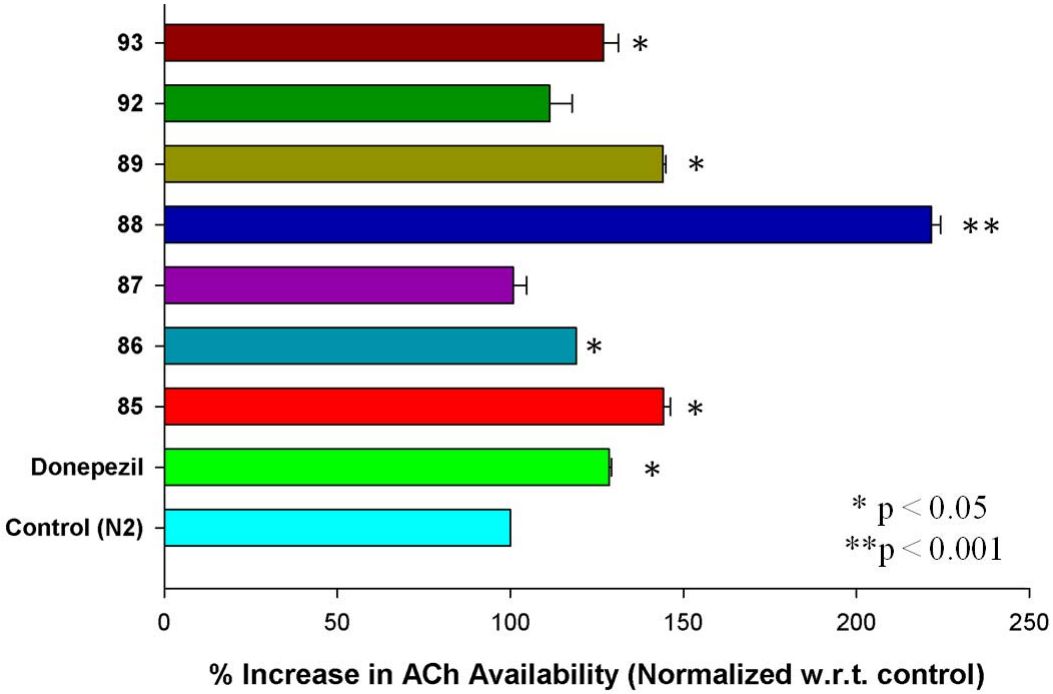

Figure 11: Effect of different compounds on the ACh availability in *C. elegans* model system.

The compounds **85** and **86** with est. AChE IC_{50} of 87.36 and 141.22 nM also showed good *in-vivo* % LI of 89.190 and 89.597 respectively at an oral dose of 20 μmol/kg (1% aqueous suspension in gum acacia). In the colorimetric assay system (Ellman method), the compound **86** showed observed AChE IC_{50} = 3310 nM. In the *C. elegans* model system, compound **85** was found to increase the level of ACh in the synaptic cleft to more extent as compared to Donepezil, a widely used anti-Alzheimer drug. The compound **87** with est. AChE IC_{50} of 313.92 nM showed the % LI of 67.395, which was found to be comparatively more potent than its homologue **88** (est. AChE IC_{50} = 441.03 nM & % LI = 33.431), the least active compound in this series. The compound **90** and **91** were also found to be potent memory enhancer with % LI of 75.979 and 61.525 respectively. Two compounds **92** and **93,** with estimated (est.) AChE IC_{50} of 99.83 and 86.50 nM respectively, showed excellent *in-vivo* anti-dementia activity with %LI of 106.768 and 123.06 respectively, at an oral dose of 20 μmol/kg (1% aqueous suspension in gum acacia) compared to the reference drug (Donepezil; % LI = 134.416; oral dose = 20 μmol/kg; observed AChE IC_{50} = 90 nM). The increase in the availability of neurotransmitter ACh in the synaptic cleft of *C. elegans* associated with these two compounds **92** and **93** was almost equal to the ACh level increased by the well known AChE inhibitor, Donepezil (Figure 11). As shown in Figure 12, the three measurements, namely % LI, % increase in ACh in the synaptic cleft, and estimated AChE IC_{50} (nM) of compounds **85**, **86**, **90-93** and Donepezil (reference drug) well corroborated with each other, in terms of trend co-linearity for all compounds except compounds **87-89**. Exact reason for such exceptions is not known and requires some additional studies. However, it may be stated that the main reason for such exceptions may be their inability to cross the blood brain barrier (BBB), because of their higher hydrophilic factor (hyd. factor) which is a measure of hydrophilic nature of a compound. The hydrophilic factor of each compound was calculated using DRAGON program.[68] The hydrophilic factor of compound **87**, **88,** and **89** was -2.87, -2.34 and -2.87 respectively, which was quite higher than rest of the

compounds (hyd. factor range: -6.87 to -8.43). Also, it may interesting to note that these three exceptional compounds (**87**-**89**) are composed of the same heterocyclic core, 1,2,3,4-tetrahydroquinoline, out of which the compounds **87** and **89** have meta- and para-bromophenyl groups respectively attached to carbamoyl nitrogen (Table 5).

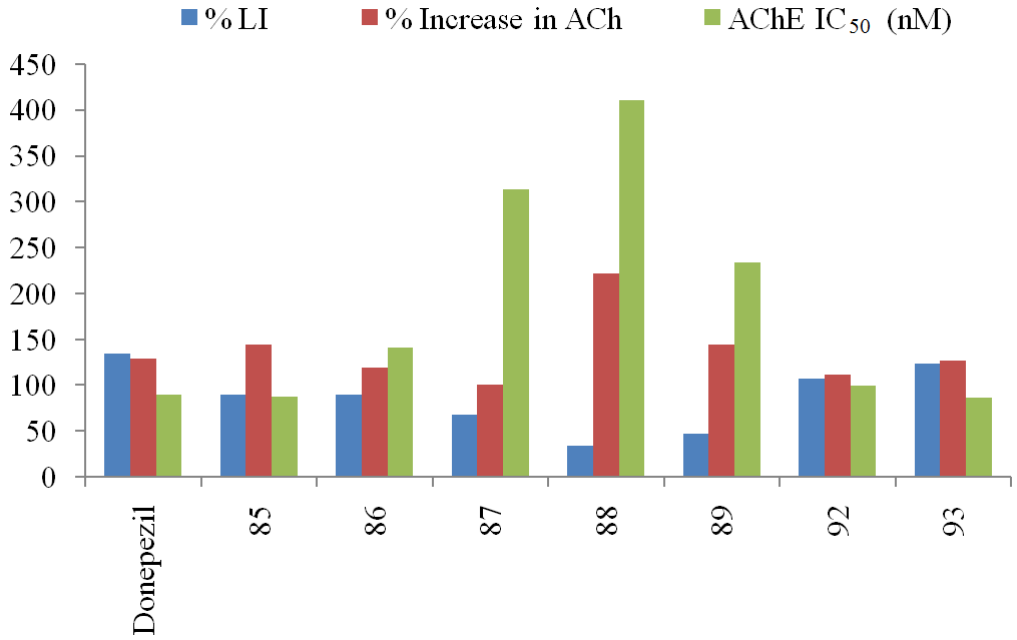

Figure 12: Comparative analysis of the biological activities of the synthesized compounds from three different assay systems.

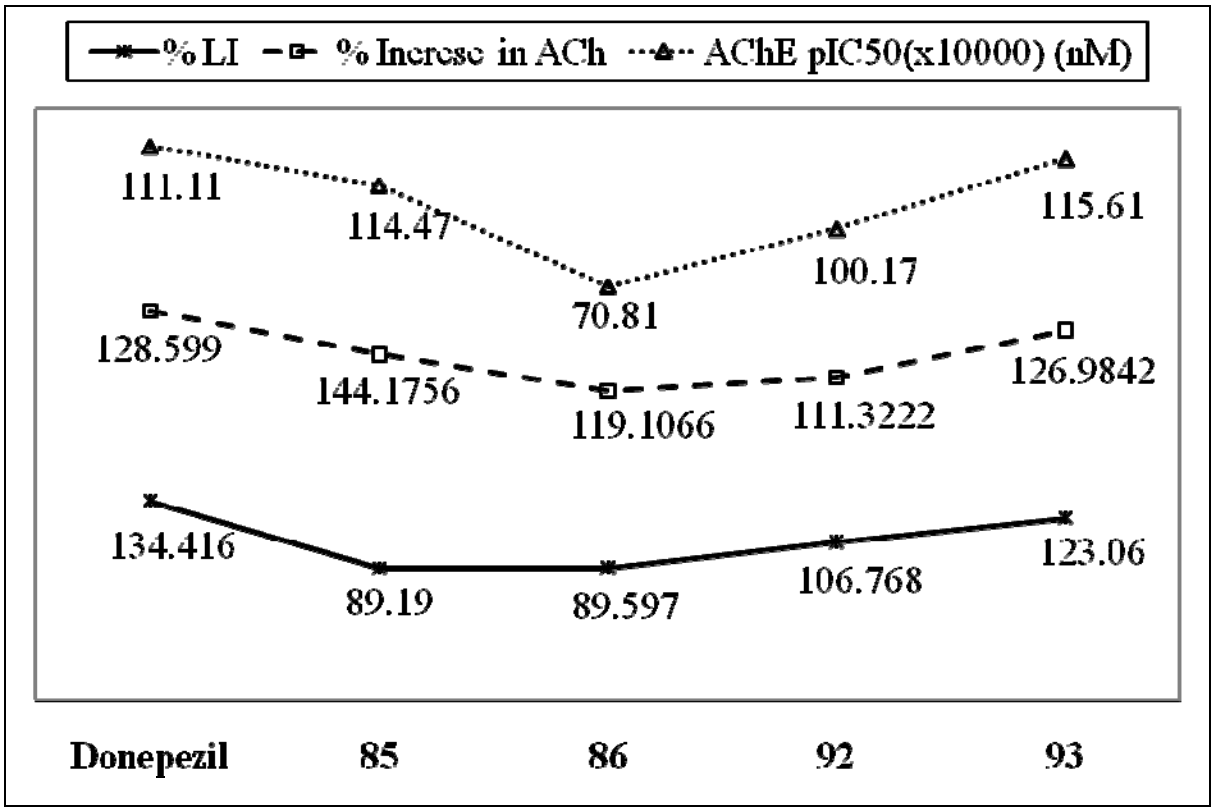

Figure 13: Stacked line plot of the estimated AChE pIC_{50} (nM), the %LI and the % increase in ACh availability associated with different compounds.

Figure 13 shows the stacked-line plot of the % LI, and % increase in ACh availability at synaptic cleft, where it is evident that these three variables, obtained from two different assay systems, are following similar trend. Also, it further proves the fact that the memory (cognition) is highly dependent on the availability of ACh in the synaptic cleft in between pre- and post-synaptic neurons. In view of it, it may be noted that the % availability of the neurotransmitter ACh in the synaptic cleft is the most determinant factor of memory functioning in a model system.

Based on the above results, obtained from three diverse assay systems, the two compounds **85** and **86** (Table 5) were selected as potential lead compounds for further consideration. These two compounds are novel substituted carbamate esters attached to 6th position of N-benzyl-1, 2, 3, 4-tetrahydroquinoline core. In our lab, further optimization of these leads is under progress to develop more comprehensive structure-activity relationship, which may lead to the discovery of potential candidate molecule as AChE inhibitors for the treatment of the AD.

Structure-Activity Relationship (SAR): The SAR analysis of a set of 9 carbamates provided important insights into the essential structural requirements for effective AChE inhibition and memory enhancement, by increasing the level of cognitive neurotransmitter ACh in the synaptic cleft. It was observed that the introduction of bulky hydrophobic groups at the carbamoyl nitrogen led to compounds with better AChEI and learning improvement (LI) activity. Among the substituted phenyl groups attached to carbamoyl nitrogen, the order of preference should be: ortho (o) > meta (m) > para (p) for AChE inhibition and memory enhancement. For example, ortho-chlorophenyl should be preferred over meta- and para-chlorophenyl, as an attachment group to the carbamoyl nitrogen. Conclusions drawn based on their structural analysis are in good agreement with our earlier published structural insights gained from the 3D-QSAR comparative molecular field analysis (CoMFA) and comparative molecular similarity indices analysis (CoMSIA) studies on diverse carbamates.[40] In this study, the presence of bulky hydrophobic groups at the carbamoyl nitrogen was found to be essential for potential AChE inhibition. On the other hand, structural analysis of the lead compounds **85** and **86** suggests the presence of a hydrophobic group with steric bulk on the nitrogen of the 1,2,3,4-tetrahydroquinoline is responsible for their potential activities, which is also well corroborates with our reported structural insights.[40]

CONCLUSION

In the present study, an efficient virtual screening has been performed using a Catalyst/HypoGen-based pharmacophore and *in-house* virtual library for discovering novel promising AChE inhibitors. The quantitative pharmacophore has been developed using the training set of 24 molecules with the help of HypoGen module implemented in the Catalyst. The best pharmacophore model provided a statistically significant correlation of 0.95 (rms = 0.568), and explained about 91% AChEI activity variation in the training set compounds. The best pharmacophore model has also well estimated AChEI activities of the test set compounds with overall predictive correlation (r) of 0.814 and explained about 71% AChEI activity variation. In addition, this model very well predicted diverse class of clinically potent AChE inhibitors. The PBVS of *in-house* virtual library using the statistically significant 3D pharmacophore model provided novel potent AChE inhibitors. The pharmacological evaluation of a set of 9 synthesized carbamates, against three diverse assay systems namely (i) *in-vitro* (Ellman method), (ii) *in-vivo* (passive avoidance test), and (iii) *Caenorhabditis elegans* model system-based aldicarb-sensitivity assay, led into the discovery of novel potent

carbamates, which are found to increase availability of acetylcholine (ACh) in the synaptic cleft by inhibiting AChE enzyme, and also found to enhance the learning tendency (memory) in Swiss male mice. Based on the data derived from three diverse assays, two novel lead compounds, namely **85** and **86,** with desirable physicochemical properties, have been selected as candidate molecules for further optimization, which in the recent future may provide novel potent AChE inhibitors for the therapy of Alzheimer's disease (AD), an unmet global need.

EXPERIMENTAL SECTION

Pharmacophore-Based Virtual Screening

Modeling Tools and Biological Data: All molecular modeling works were accomplished using the Window-based Accelrys Discovery Studio version 2.0 (DS2.0).[69] The Catalyst 4.7 was used for pharmacophore modelling and virtual screening.[69] A structurally diverse set of 64 compounds, reported as AChE inhibitors with AChE inhibitory activity data (expressed as IC_{50}) spanning about 3.6 orders of magnitude (10-41130 nM), were considered in the present study.[70-74] The AChE inhibitors were categorized into highly active (AChE $IC_{50} \leq 100$ nM), moderately active ($100 < IC_{50} < 500$ nM), and poorly active (AChE $IC_{50} \geq 500$ nM). The dataset was classified into the training set (24 compounds: Figure 1) and test set (40 compounds) in such a way to avoid any redundancy in terms of structural features or activity range and also to provide clear and concise information during model development using the HypoGen algorithm implemented in the Catalyst software.[75]

The pharmacophore model development methodology is well described in the literature.[76, 77] In brief, the energy minimized 3D structures (using CharmM forcefield[78] until the gradient dropped below 0.001) were submitted for diverse conformational generation using the "best quality" conformational search option in the Catalyst software using a constraint of 20 kcal/mol energy threshold above the global energy minimum, 255 as the maximum number of conformations and CharmM force field parameters[78] to ensure maximum coverage in the conformational space. All other settings were kept as default. On the basis of the structural characteristics of the training set compounds, only HBA, HBD, HY, RA features from feature dictionary were considered for model development. The pharmacophore modeling, which is done in three subsequent phases *viz.* constructive, subtractive and optimization phases, was accomplished using HypoGen algorithm based on the training set of 24 compounds. The top 10 scoring pharmacophore models (hypotheses) were analysed for their statistical significance and to determine the best model by analysing quality of the mapped conformations as well as analysis of theoretical costs, namely fixed, null, total, error, weight, configuration, and residual costs.[79] The term 'cost' in HypoGen algorithm indicates the number of binary bits required to generate a particular pharmacophore/hypothesis. The recommended values of residual, weight and configuration costs are ≥ 40, ≤ 2 and ≤ 17 respectively. Further quality assessment and validation of the pharmacophore model was done using the test set compounds, which were kept apart during the model development process.

In vitro Pharmacology: Ellman Method

The assay of AChE inhibition was performed according to method described by Ellman *et al.*[65] using the human AChE purified from red blood cells. The kinetic profile of the AChE enzyme activity was studied spectrophotometrically at a wavelength of 412 nM at an interval of 15s. The assay for each sample was run in duplicate and each experiment was performed thrice. The test substance was incubated with enzyme in the concentration of 100 µg/mL of reaction mixture for 30 min at 37^{o}C prior to obtaining the kinetic profile of AChE activity. Donepezil (1µg/mL) was used as standard AChE inhibitor (standard control). The AChE inhibitory activity was calculated on the basis of % decrease from control values i.e. AChE activity without incubation with any standard or test drug.

In vivo Pharmacology:

Passive Avoidance Test: The study was conducted in adult Swiss male mice of 3-4 months (wt. 20-25 g) were kept in standard housing condition with 12h light and dark cycle. The food and water were available *ad libitum*. Mice were subjected to single trial passive avoidance test as described by Brioni.[66] Passive avoidance test was studied in a computerized shuttle box (Columbus Instruments, Ohio, USA) provided with a software programme PACS 30. The shuttle box is comprised of two compartments isolated by an automated door. After exploration period of 30s for acclimatization, animal was subjected to a trial of 270s. Each mouse was placed in the bright compartment and on transfer into the dark compartment; it was given an electric shock (0.5 mA for 5 s) through floor grid. Transfer of mice from bright to dark compartment was recorded as transfer latency time (TLT) in seconds. TLT was recorded in control and treated groups (1st Trial, acquisition) and then after 24 hrs (2nd Trial, retention). An increase in the TLT on 2nd Trial (retention) as compared to 1st Trial (acquisition) was taken as the criterion for successful learning and memory improvement (cognitive activity). Mean values and standard errors (S.E.) of the mean were calculated for TLT and specific activity of AChE in the different regions of brain samples of each group. The significance of difference between values of AChE activity and TLT between the groups was determined by one-way ANOVA test that followed by Dunnett's test.

Assay employing *C. elegans* (model system): In order to study the effect of test compounds on ACh release, a biological assay employing model system *C. elegans*,[44] was performed as per the method described in Mahoney *et al.*[46] with slight modifications. Briefly, the wild type strain N2 (var. Bristol) of *C. elegans,* procured from *C. elegans* Genetics Center (CGC) University of Minnesota, USA, was used. Healthy gravid population of nematodes grown on Nutrient Growth Medium (NGM) Agar under standard conditions[80] (Brenner, 1974) were subjected to embryo isolation by axenization method[81] (Stiernagle, 1999). Embryos were transferred to NGM plates seeded with their standard food (bacteria *E. coli)* premixed with the test compounds. Nematodes were grown under standard conditions on the treated plates for 48 hours and then washed off the plates, pelletted and transferred to assay plates containing Aldicarb at a concentration of 1mM premixed with NGM. Assays were performed in duplicates and the percentage of worms paralyzed at a time point of 3 hours was recorded. The percentage of worms paralyzed under treated conditions was normalized against control values and the data was analyzed for Mean ± S.E; statistical significance of data was calculated by Students t-test using Sigma Stat software package.

Chemistry: General methods: Reagents were purchased from common commercial suppliers and were used without further purification. Solvents were purified and dried by standard procedures, when necessary. Chromatographic separations of the synthesized intermediates and title compounds were performed on silica gel (Merck: 100-200 mesh). Thin-layer chromatography was used to monitor the reactions. Melting points (uncorrected) were determined with Büchi 510 apparatus. Characterization of the synthesized compounds was accomplished in the Sophisticated Analytical Instrument Facility (SAIF) department of CDR, Lucknow. IR spectroscopy was carried out using Perkin-Elmer 881 spectrophotometer and the values are expressed as ν_{max} cm^{-1}. Mass spectra (MS) were recorded on a Jeol (Japan) SX 102/DA-6000 Mass Spectrometer. ^1H NMR spectra were recorded on Bruker Spectrospin spectrometer at 300 MHz. The chemical shifts are reported in δ scale (ppm) and are relative to tetramethyl silane (TMS) as internal standard. The coupling constants *J* are given *Hertz* and spin multiplicities are expressed s (singlet), d (doublet), t (triplet), dd (double doublet), qunit (quintet) and m (multiplet). Elemental analyses were performed on a Carlo Erba Model EA-1108 elemental analyzer and data of C, H and N are within ±0.4% of calculated values. All reported title compounds were assessed to be ≥95% pure by analytical HPLC method.

Carbamylation: Method A: Synthesis of Hexylcarbamic acid 1-benzyl-1,2,3,4-tetrahydroquinolin-6-yl ester (85): A mixture of 1-benzyl-1,2,3,4-tetrahydroquinolin-6-ol

(**83,** 0.239 g, 0.001 mol), hexyl isocyanate (0.152 g, 0.0012 mmol) and pyridine (0.5 mL) in dry THF (10 mL) was heated with stirring at 65°C for 72 hours. After the completion, the reaction mixture was cooled and quenched with water (1 mL) and concentrated under vacuum. The separated solid was washed with water (2x3 mL) and crystallized with anhydrous ether to give the title product **85**. Yield: 0.30 g (81.9%), m.p. >335°C. ^{1}H NMR ($CDCl_3$, 200 MHz): δ 0.89 (bs, 3H), 0.90-1.29 (m, 4H), 1.50-1.56 (m, 4H), 1.98-2.15 (m, 2H), 2.79 (t, *J*=6.21 Hz, 2H), 3.17-3.36 (m, 4H), 4.44 (s, 2H), 4.88 (bs, 1H), 6.42 (d, *J*=8.72 Hz,1H), 6.67-6.75 (m, 2H), 7.22-7.35 (m, 5H). FTIR (KBr): cm^{-1} 669, 760, 1026, 1217, 1348, 1501, 1615, 1728, 2402, 2857, 3018, 3450. EIMS: m/z 366 (M^+). HR-MS: calcd for $C_{23}H_{30}N_2O_2$ (M^+) 366.2307; found 366.2342.

Method B: Synthesis of 2-Chlorophenylcarbamic acid 1-benzyl-1,2,3,4-tetrahydroquinolin-6-yl ester (86): A solution of 1-benzyl-1,2,3,4-tetrahydroquinolin-6-ol (**83**, 0.239 g, 0.001 mol) in dry ether (10 mL) was added to a stirred suspension of sodium hydride (0.024 g, 0.001 mol) in dry THF (15 mL) at -10°C during 10 minutes. The reaction mixture was stirred for an additional 20 minutes. 2-chlorophenyl isocyanate (0.184 g, 0.001 mol) was added to the stirring reaction mixture. The stirring was continued for an additional 2 hours during which the temperature was allowed to rise to 35°C. The reaction mixture was quenched with water (0.2 mL), concentrated under vacuum, diluted with water (5 mL), extracted with chloroform (2x5 mL) and dried over sodium sulphate. The combined fractions of chloroform were concentrated under vacuum. The residue was chromatographed on silica gel column using chloroform: hexane (20:80) as eluent to give the title product **86** (0.25g, 63.7%). m.p. 130-133°C. ^{1}H NMR ($CDCl_3$, 200 MHz): δ 1.90-2.02 (m, 2H), 2.82 (t, *J*=6.18 Hz, 2H), 3.30-3.35 (m, 2H), 4.46 (s, 2H), 6.43-6.48 (m, 1H), 6.74-6.82 (m, 2H), 7.20-7.25 (m, 5H), 7.44-7.46 (m, 4H). FTIR (KBr): cm^{-1} 534, 754, 807, 882, 1018, 1059, 1193, 1245, 1303, 1352, 1432, 1506, 1597, 1718, 1749, 2371, 2830, 2922, 3418, 3760. EIMS: m/z 393 $(M+1)^+$. HR-MS: calcd for $C_{23}H_{21}ClN_2O_2$ $(M+1)^+$ 393.1292; found 393.1312.

General Procedure of Debenzylation: Synthesis of 3-bromophenylcarbamic acid 1,2,3,4-tetrahydroquinolin-6-yl ester (87): A nitrogen flushed mixture of 3-bromophenylcarbamic acid 1-benzyl-1,2,3,4-tetrahydroquinolin-6-yl ester (0.218 g, 0.005 mol, Note: This compound was synthesized using the method A used for synthesis of compound 85) and 5% Pd-C (0.02 g) in absolute ethanol (25 mL) was shaken in a par apparatus at 38°C under 50 psi pressure of hydrogen for 4 hours. Pd-C was then discarded through filtration. The reaction mixture was concentrated under vacuum and the residue was washed with dichloromethane (2x3 mL) to give the title product **87** (0.16 g, 92.4%). m.p. 196-198°C. ^{1}H NMR (DMSO-d_6, 200 MHz): δ 1.73-1.81 (m, 2H), 2.55 (t, *J*=6.34 Hz, 2H), 3.06 (t, *J*=5.58 Hz, 2H), 6.67-6.98 (m, 4H), 6.90-7.20 (m, 2H), 7.36 (bs, 1H), 9.39 (bs, 1H). FTIR (KBr): cm^{-1} 509, 694, 758, 815, 886, 1012, 1084, 1149, 1216, 1319, 1352, 1442, 1504, 1549, 1600, 1710, 2365, 2479, 2727, 2827, 2927, 3420, 3780. EIMS: m/z 347 $(M+1)^+$. HR-MS: calcd for $C_{16}H_{15}BrN_2O_2$ $(M+1)^+$ 347.0317; found 347.0322.

4-chloro-3-trifluoromethylphenylcarbamic acid 1,2,3,4-tetrahydroquinolin-6-yl ester (88): This compound was synthesized using the same debenzylation procedure used for the compound 87 taking a nitrogen flushed mixture of 4-chloro-3-trifluoromethylphenylcarbamic acid 1-benzyl-1, 2, 3, 4-tetrahydroquinolin-6-yl ester (0.23 g, 0.005 mol) and 5% Pd-C (0.02 g) in absolute ethanol (20 mL). The 4-chloro-3-trifluoromethylphenylcarbamic acid 1-benzyl-1, 2, 3, 4-tetrahydroquinolin-6-yl ester was synthesized using the method B. Yield: 0.16 g (86.4. %), m.p. 150-151°C. ^{1}H NMR (DMSO-d_6, 200 MHz): δ 1.89-1.95 (m, 2H), 2.76 (t, *J*=6.08 Hz, 2H), 3.28 (t, 2H, *J*=5.52 Hz), 6.44-6.49 (m,1H), 6.72-6.75 (m, 2H), 7.37- 8.00 (m, 2H), 10.14 (bs, 1H). FTIR (KBr): cm^{-1} 661, 698, 769, 796, 819, 892, 944, 1023, 1072, 1147, 1217, 1290, 1347, 1384, 1424, 1450, 1506, 1599, 1707, 1740, 2364, 2489, 2837, 2950, 3359,

3773, 3888. EIMS: m/z 371 $(M+1)^+$. HR-MS: calcd for $C_{17}H_{14}ClF_3N_2O_2$ $(M+1)^+$ 371.0696; found 371.0681

4-bromophenylcarbamic acid 1,2,3,4-tetrahydroquinolin-6-yl ester (89): This compound was synthesized using the same debenzylation procedure used for the compound 87 taking a nitrogen flushed mixture of 4-bromophenylcarbamic acid 1-benzyl-1,2,3,4-tetrahydroquinolin-6-yl ester (0.655 g, 0.0015 mol) and 5% Pd-C (0.06 g) in absolute ethanol (20 mL). The 4-bromophenylcarbamic acid 1-benzyl-1,2,3,4-tetrahydroquinolin-6-yl ester was synthesized using the method B. Yield: 0.48 g (92.3 %), m.p. 197-199°C. ^{1}H NMR (DMSO-d_6, 200 MHz): δ 1.82-2.00 (bs, 2H), 2.76 (t, *J*=6.22 Hz, 2H), 3.27 (t, *J*=5.26 Hz, 2H), 7.01-7.08 (m, 3H), 7.25-7.39 (m, 4H), 10.14 (s, 1H). FTIR (KBr): cm^{-1} 506, 608, 690, 749, 814, 884, 927, 1005, 1211, 1265, 1319, 1354, 1401, 1440, 1501, 1550, 1601, 1748, 1938, 2370, 2779, 2725, 2767, 2823, 2922, 3262, 3420, 3774. EIMS: m/z 348 $(M+1)^+$. HR-MS: calcd for $C_{16}H_{15}BrN_2O_2$ $(M+1)^+$ 347.0317; found 347.0338.

4-Chloro-3-trifluoromethylphenylcarbamic acid 1-methyl-1,2,3,4-tetrahydro quinolin-6-yl ester (90): This compound was synthesized using the general carbamoylation method B taking a solution of 1-methyl-1, 2, 3, 4-tetrahydroquinolin-6-ol (**84**, 0.326 g, 0.002 mol) in dry THF (5 mL), a suspension of sodium hydride (0.048 g, 0.002 mol) in dry THF (5 mL) at -10°C and 4-chloro-3-trifluoromethylphenyl isocyanate (0.53, 0.002 mol). Yield: 0.52g (67.6%), m.p. 151-152°C. ^{1}H NMR ($CDCl_3$, 200 MHz): δ 1.94-2.00 (m, 2H), 2.76 (t, *J*=6.50 Hz, 2H), 2.87 (s, 3H), 3.20 (t, *J*=5.63 Hz, 2H), 6.52-6.57 (m, 1H), 6.78-6.82 (m, 2H), 7.46-7.81 (m, 3H). FTIR (KBr): cm^{-1} 537, 666, 756, 831, 894, 1029, 1147, 1264, 1423, 1489, 1542, 1596, 1698, 1741, 2373, 2928, 3118, 3232, 3402; 3687, 3760. EIMS: m/z: 384 (M^+). HR-MS: calcd for $C_{18}H_{16}ClF_3N_2O_2$ (M^+) 384.0852; found 384.0865.

4-bromophenylcarbamic acid 1-methyl-1,2,3,4-tetrahydroquinolin-6-yl ester (91): This compound was synthesized using the general carbamoylation method B using a solution of 1-methyl-1, 2, 3, 4-tetrahydroquinolin-6-ol (**84**, 0.326 g, 0.002 mol) in dry THF (5 mL) , a suspension of sodium hydride (0.048 g, 0.002 mol) in dry THF (5 mL) at -10°C and 4-bromo-phenyl isocyanate (0.734, 0.002 mol). Yield: 0.40g (52.3%), m.p. 155-159°C. ^{1}H NMR ($CDCl_3$, 200 MHz): δ 1.94-2.03 (m, 2H), 2.76 (t, *J*=6.42 Hz, 2H), 2.87 (s, 3H), 3.20 (t, *J*=5.64 Hz, 2H), 6.52-6.57 (m, 1H), 6.78-6.88 (m, 2H), 7.25-7.45 (m, 4H). FTIR (KBr): cm^{-1} 674, 774, 1020, 1365, 1590, 2366, 2834, 2934, 3433, 3757, 3867, 3906. EIMS: m/z 361$(M+1)^+$. HR-MS: calcd for $C_{17}H_{17}BrN_2O_2$ $(M+1)^+$ 361.0473; found 361.0469.

n-heptylcarbamic acid quinolin-6-yl ester (92): This compound was synthesized using the method A using a mixture of quinolin-6-ol (**82**, 0.29 g, 0.002 mol), heptyl isocyanate (0.39 mL, 0.0024 mol) and pyridine (2 mL) in dry THF (10 mL). Yield: 0.30 g (52.4%). m.p. 77-80°C. ^{1}H NMR ($CDCl_3$, 200 MHz): δ 0.88 (bs, 3H), 1.33-1.34 (m, 8H), 1.57-1.62 (m, 2H), 3.25-3.35 (m, 2H) 5.10 (s, 1H), 7.36-7.52 (m,1H), 7.47-7.52 (m, 1H), 7.60-7.61 (m, 1H), 8.07-8.12 (m, 2H), 8.86-8.88 (m, 1H). FTIR (KBr): cm^{-1} 478, 648, 731, 771, 838, 910, 977, 1024, 1157, 1215, 1363, 1464, 1498, 1532, 1600, 1719, 2371, 2861, 2944, 3022, 3359, 3762. FAB-MS: m/z: 287 $(M+1)^+$. HR-MS: calcd for $C_{17}H_{22}N_2O_2$ $(M+1)^+$ 287.1681; found 287.1698.

2-chlorophenylcarbamic acid quinolin-6-yl ester: This compound was synthesized using the method A using a mixture of quinolin-6-ol (**82**, 0.29 g, 0.002 mol), 2-chloro-phenyl isocyanate (0.33 mL, 0.0024 mmol) and pyridine (0.3 mL) in dry tetrahydrofuran (5 mL). Yield: 0.30 g (50.2%), m.p. 225-228°C. ^{1}H NMR (Pyridine-d_5, 200 MHz): δ 6.96-7.57 (m, 9H), 8.62-8.71 (m, 1H), 9.47 (m, 1H). FTIR (KBr): cm^{-1} 903, 943, 1040, 1230, 1291, 1353, 1437, 1474, 1552, 1592, 1646, 2373, 3289, 3759. EIMS: m/z: 298 $(M)^+$. HR-MS: calcd for $C_{16}H_{11}ClN_2O_2$ $(M)^+$ 298.0509; found 298.0544.

Molecular Docking:

The GOLD[53] program was used for calculating the docking modes of the compounds **1**, **65**, **86** and **93** into the binding site of AChE enzyme. Atomic coordinates of AChE enzyme was obtained from the crystal structure of AChE in complex with rivastigmine (PDB Id: 2GQR[51]). The protein was prepared using *Protein Preparation Wizard* implemented in Schrödinger software,[63] where waters and rivastigmine were removed from the PDB file, and the polar hydrogen atoms were added to the amino acid residues before the docking study.

Covalent docking: Covalent docking is a unique feature of GOLD program, which is able to dock covalently bound inhibitors. Both protein (AChE) and ligand files were set up with the Ser200 oxygen (O, link atom), which was assigned in both the protein and ligand input files. The GOLD program assumes that there is just one atom linking the ligand to the protein (*e.g.* the O in a serine residue). More details about this docking method (http://www.ccdc.cam.ac.uk/products/life_sciences/gold/).

Acknowledgments:
The authors (SSC and KKR) are thankful to the Council of Scientific and Industrial Research, New Delhi for the financial assistance in the form of a fellowship and to Sophisticated Analytical Instrument Facility (SAIF) department of Central Drug Research Institute, Lucknow for the characterization of compounds. The technical assistance of Mr. A. S. Kushwaha, Zahid Ali and Dayanand Vishwakarma is also acknowledged.

Supporting Information Available: Synthetic procedures, characterization (NMR, MASS, IR and elemental analysis) data of the key intermediates **79-84,** and the overlay of compounds (**65-76, 85-93**) over the best pharmacophore (Hypo-01). This material is available free of charge *via* the Internet at http://www.pubs.acs.org.

References

1. Butters, N.; Delis, D. C.; Lucas, J. A. Clinical Assessment of Memory Disorders in Amnesia and Dementia. *Annu. ReV. Psychol.* **1995**, *46*, 493–523.
2. (a) Cummings, J. L.; Doody, R.; Clark, C. Disease-modifying Therapies for Alzheimer Disease: Challenges to Early Intervention. *Neurology* **2007**, *69*, 1622–1634. (b) Giacobini, E. Cholinesterases: New Roles in Brain Function and in Alzheimer's disease. *Neurochem. Res*. **2003**, *28*, 515–522. (c) Terry, A. V.; Buccafusco, J. J. The Cholinergic Hypothesis of Age and Alzheimer's Disease-related Cognitive Deficits: Recent Challenges and Their Implications for Novel Drug Development. *J. Pharmacol. Exp. Ther.* **2003**, *306*, 821–827.
3. Bazelyansky, M.; Robey, E.; Kirsch, J. F. Fractional Diffusion-Limited Component of Reactions Catalyzed by Acetylcholinesterase. *Biochemistry* **1986**, *25*, 125–130.
4. Ballmaier, M.; Casamenti, F.; Scali, C.; Mazzoncini, R.; Zoli, M. Rivastigmine Antagonizes Deficits in Prepulse Inhibition Induced by Selective Immunolesioning of Cholinergic Neurons in Nucleus Basalis Magnocellularis. *Neuroscience* **2002**, *114*, 91–98.
5. Barnes, C. A.; Meltzer, J.; Houston, F.; Orr, G.; McGann, K. Chronic Treatment of Old Rats with Donepezil or Galantamine: Effects on Memory, Hippocampal Plasticity and Nicotinic Receptors. *Neuroscience* **2000**, *99*, 17–23.
6. Van Dam, D.; Abramowski, D.; Staufenbiel, M.; De Deyn, P. P. Symptomatic Effect of Donepezil, Rivastigmine, Galantamine and Memantine on Cognitive Deficits in the APP23 Model. *Psychopharmacology* **2005**, *180*, 177–190.

7. Clegg, A.; Bryant, J.; Nicholson, T.; McIntyre, L.; De Broe, S.; Gerard, K.; Waugh, N. Clinical and Cost-Effectiveness of Donepezil, Rivastigmine and Galantamine for Alzheimer's Disease: A Rapid and Systematic Review. *Health Technol. Assess.* **2001**, *5*, 1–137.
8. Clegg, A.; Bryant, J.; Nicholson, T.; McIntyre, L.; De Broe, S.; Gerard, K.; Waugh, N. Clinical and Cost-effectiveness of Donepezil, Rivastigmine and Galantamine for Alzheimer's Disease. *Int. J. Technol. Assess. Health Care* **2002**, *18*, 497–507.
9. Goldlist, B.; Gordon, M.; Naglie, G. Galantamine vs Donepezil in the Treatment of Alzheimer's disease. *Drugs Aging* **2003**, *20*, 1139–1140.
10. Prasher, V. P. Review of Donepezil: Ageing and Health Issues in Intellectual Disabilities. *Int. J. Geriatr. Psychiatry* **2004**, *19*, 509–515.
11. Frantz, S. Drug Discovery: Playing Dirty. *Nature* **2005**, *437*, 942–943.
12. Van der Schyf, C. J.; Youdim, M. B. Multifunctional Drugs as Neurotherapeutics. *Neurotherapeutics* **2009**, *6*, 1–3.
13. Scarpini, E.; Scheltens, P.; Feldman, H. Tretament of Alzheimer's Disease: Current Status and New Perspectives. *Lancet Neurol.* **2003**, *2*, 539–547.
14. Tariot, P. N.; Federoff, H. J. Current treatment for Alzheimer disease and future prospects. *Alzheimer Dis. Assoc. Disord.* **2003**, *17* (suppl 4), S105–S113.
15. Aracava, Y.; Pereira, E. F. R.; Maelicke, A.; Albuquerque, E. X. Memantine Blocks {alpha}7* Nicotinic Acetylcholine Receptors More Potently than N-methyl-D-aspartate Receptors in Rat Hippocampal Neurons. *J. Pharmacol. Exp. Ther.* **2005**, *312*, 1195–1205.
16. Banerjee, P.; Samoriski, G.; Gupta, S. Comments on " Memantine Blocks {alpha}7* Nicotinic Acetylcholine Receptors More Potently than N-methyl-D-aspartate Receptors in Rat Hippocampal Neurons ". *J. Pharmacol. Exp. Ther.* **2005**, *313*, 928–929.
17. Ballmaier, M.; Casamenti, F.; Scali, C.; Mazzoncini, R.; and Zoli, M. Rivastigmine Antagonizes Deficits in Prepulse Inhibition Induced by Selective Immunolesioning of Cholinergic Neurons in Nnucleus Basalis Magnocellularis. *Neuroscience* **2002**, *114*, 91–98.
18. Barnes, C. A.; Meltzer, J.; Houston, F.; Orr, G.; and McGann, K. Chronic Treatment of Old Rats with Donepezil or Galantamine: Effects on Memory, Hippocampal Plasticity and Nicotinic Receptors. *Neuroscience* **2000**, *99*, 17–23.
19. Van Dam, D.; Abramowski, D.; Staufenbiel, M.; and De Deyn, P. P. Symptomatic Effect of Donepezil, Rivastigmine, Galantamine and Memantine on Cognitive Deficits in the APP23 Model. *Psychopharmacology* (Berl) **2005**, *180*, 177–190.
20. Sussman, J. L.; Harel, M.; Frolow, F.; Oefner, C.; Goldman, A.; L, L. T.; Silman, I. Atomic Structure of Acetylcholinesterase from Torpedo californica: a Prototypic Acetylcholine-Binding Protein. *Science* **1991**, *253*, 872–879.
21. (a) Tumiatti, V.; Milelli, A.; Minarini, A.; Rosini, M.; Bolognesi, M. L.; Micco, M.; Andrisano, V.; Bartolini, M.; Mancini, F.; Recanatini, M.; Cavalli, A.; Melchiorre, C. Structure-Activity Relationships of Acetylcholinesterase Noncovalent Inhibitors Based on a Polyamine Backbone. 4. Further Investigation on the Inner Spacer. *J. Med. Chem.* **2008**, *51*, 7308–7312. (b) Bolognesi, M. L.; Cavalli, A.; Valgimigli, L.; Bartolini, M.; Rosini, M.; Andrisano, V.; Recanatini, M.; Melchiorre, C. Multi-Target-Directed Drug Design Strategy: From a Dual Binding Site Acetylcholinesterase Inhibitor to a Trifunctional Compound Against Alzheimer's Disease. *J. Med. Chem.* **2007**, *50*, 6446–6449. (c) Hardy, J.; Selkoe, D. J. The Amyloid Hypothesis of Alzheimer's Disease: Progress and Problems on the Road to Therapeutics. *Science* **2002**, *297*, 353–356.

22. Ordentlich, A.; Barak, D.; Kronman, C.; Flashner, Y.; Leitner, M.; Segall, Y.; Ariel, N.; Cohen, S.; Velan, B.; Shafferman, A. Dissection of the Human Acetylcholinesterase Active Center Determinants of Substrate Specificity. Identification of Residues Constituting the Anionic Site, the Hydrophobic Site, and the Acyl Pocket. *J. Biol. Chem.* **1993**, *268*, 17083–17095.
23. Radic, Z.; Gibney, G.; Kawamoto, S.; MacPhee-Quigley, K.; Bongiorno, C.; Taylor, P. Expression of Recombinant Acetylcholinesterase in a Baculovirus System: Kinetic Properties of Glutamate 199 Mutants. *Biochemistry* **1992**, *31*, 9760–9767.
24. (a) Amit, T.; Avramovich-Tirosh, Y.; Youdim, M. B.; Mandel, S. Targeting Multiple Alzheimer's Disease Etiologies with Multimodal Neuroprotective and Neurorestorative Iron Chelators. *FASEB J.* **2008**, *22*, 1296-1305. (b) Cavalli, A.; Bolognesi, M. L.; Minarini, A.; Rosini, M.; Tumiatti, V.; Recanatini, M.; Melchiorre, C. Multi-Target-Directed Ligands to Combat Neurodegenerative Diseases. *J. Med. Chem.* **2008**, *51*, 347- 372.
25. Soreq, H.; Seidman, S. Acetylcholinesterase: New Roles for an Old Actor. *Nat. Rev. Neurosci.* **2001**, *2*, 8–17.
26. Johnson, G.; Moore, S. W. The Adhesion Function on Acetylcholinesterase is Located at the Peripheral Anionic Site. *Biochem. Biophys. Res. Commun.* **1999**, *258*, 758–762.
27. Giacobini, E. Cholinesterases: New Roles in Brain Function and in Alzheimer's Disease. *Neurochem. Res.* **2003**, *28*, 515–522.
28. Munõz, F. J.; Aldunate, R.; Inestrosa, N. C. Peripheral Binding Site is Involved in the Neurotrophic Activity of Acetylcholinesterase. *NeuroReport* **1999**, *26*, 3621–3625.
29. Sharma, K. V.; Koenigsberger, C.; Brimijoin, S.; Gigbee, J. W. Direct Evidence for an Adhesive Function in the Noncholinergic Role of Acetylcholinesterase in Neurite Outgrowth. *J Neurosci. Res.* **2001**, *63*, 165–175.
30. Blasina, M. F.; Faria, A. C.; Gardino, P. F.; Hokoc, J. N.; Almeida, O. M.; de Mello, F. G.; Arruti, C.; Dajas, F. Evidence of Noncholinergic Function of Acetylcholinesterase During Development of Chicken Retina as Shown by Fasciculin. *Cell Tissue Res.* **2000**, *299*, 173–184.
31. Munoz-Torrero, D. Acetylcholinesterase Inhibitors as Disease Modifying Therapies for Alzheimer's Disease. *Curr. Med. Chem.* **2008**, *15*, 2433–2455.
32. Zhang, H. Y.; Yan, H.; Tang, X. C. Non-Cholinergic Effects of Huperzine A: Beyond Inhibition of Acetylcholinesterase. *Cell. Mol. Neurobiol.* **2008**, *28*, 173–183.
33. Inestrosa, N. C.; Alvarez, A.; Calderon, F. Acetylcholinesterase is a Senile Plaque Component that Promotes Assembly of Amyloid Beta-Peptide into Alzheimer's Filaments. *Mol. Psychiatry* **1996**, *1*, 359–361.
34. De Ferrari, G. V.; Canales, M. A.; Shin, I.; Weiner, L. M.; Silman, I.; Inestrosa, N. C. A Structural Motif of Acetylcholinesterase that Promotes Amyloid Beta-Peptide Fibril Formation. *Biochemistry* **2001**, *40*, 10447–10457.
35. Bartolini, M.; Bertucci, C.; Cavrini, V.; Andrisano, V. Amyloid Aggregation Induced by Human Acetylcholinesterase: Inhibition Studies. *Biochem. Pharmacol.* **2003**, *65*, 407–416.
36. Klebe, G.; Abraham, U.; Mietzner, T. Molecular Similarity Indices in a Comparative Analysis (CoMSIA) of Drug Molecules to Correlate and Predict Their Biological Activity. *J. Med. Chem.* **1994**, *37*, 4130–4146.
37. Klebe, G.; Abraham, U. Comparative Molecular Similarity Index Analysis (CoMSIA) to Study Hydrogen-Bonding Properties and to Score Combinatorial Libraries. *J. Comput.-Aided Mol. Des.* **1999**, *13*, 1–10.
38. Catalyst, release Version 4.1; Accelrys Inc.: San Diego, CA 2006.

39. Chaudhaery, S. S.; Roy, K. K.; Saxena, A. K. Consensus Superiority of the Pharmacophore-Based Alignment, Over Maximum Common Substructure (MCS): 3D-QSAR Studies on Carbamates as Acetylcholinesterase Inhibitors. *J. Chem. Inf. Model.* **2009,** *49,* 1590–1601.
40. Roy, K. K.; Dixit, A.; Saxena, A. K. An Investigation of Structurally Diverse Carbamates for Acetylcholinesterase (AChE) Inhibition using 3D-QSAR Analysis. *J. Mol. Graph. Model.* **2008**, *27*, 197-208.

41. Lopez-Rodriguez, M. L.; Benhamu, B.; de la Fuente, T.; Sanz, A.; Pardo, L. A Three-Dimensional Pharmacophore Model for 5-Hydroxytryptamine 6 (5-HT6) Receptor Antagonists. *J. Med. Chem.* **2005**, *48*, 4216–4219.
42. Güner, O.; Clement, O.; Kurogi, Y. Pharmacophore Modeling and Three Dimensional Database Searching for Drug Design Using Catalyst: Recent Advances. *Curr. Med. Chem.* **2004**, *11*, 2991–3005.
43. Kim, H. -J.; Doddareddy, M. R.; Choo, H.; Cho, Y. S. No, K. T.; Park, W. K.; Pae, A. N. New Serotonin 5-HT6 Ligands from Common Feature Pharmacophore Hypotheses. *J. Chem. Inf. Model.* **2008,** *48*, 197–206.
44. (a) Riddle, D. L. *C. elegans* II. Cold Spring Harbor Laboratory Press: Plainview, N.Y. 1997. (b) Kaletta, T.; Hengartner, M. O. Finding function in novel targets: C. elegans as a model organism. Nat. Rev. Drug. Discov. **2006**, *5*, 387–398.
45. Sieburth, D.; Ch'ng, Q.; Dybbs, M.; Tavazoie, M.; Kennedy, S.; Wang, D.; Dupuy, D.; Rual, J. F.; Hill, D. E.; Vidal, M.; Ruvkun, G.; Kaplan, J. M. Systematic analysis of genes required for synapse structure and function. *Nature* **2005**, *436*, 510–517.
46. Mahoney, T. R.; Luo, S.; Nonet, M. L. Analysis of synaptic transmission in *Caenorhabditis elegans* using an aldicarb-sensitivity assay. *Nat. Protoc.* **2006**, *1*, 1772–1777.
47. Nguyen, M.; Alfonso, A.; Johnson, C. D.; Rand, J. B. *Caenorhabditis elegans* mutants resistant to inhibitors of acetylcholinesterase. *Genetics* **1995**, *140*, 527–535.
48. Debnath, A. K. Generation of Predictive Pharmacophore Models for CCR5 Antagonists: Study with Piperidine- and Piperazine-Based Compounds as a New Class of HIV-1 Entry Inhibitors. *J. Med. Chem.* **2003**, *46*, 4501–4515.
49. Hirashima, A.; Shigeta, Y.; Eiraku, T.; Kuwano, E. Inhibitors of Calling Behavior of *Plodia interpunctella*. *J. Insect Sci.* **2003**, *3*, 4−13.
50. Xu, Y.; Colletier, J. -P.; Weik, M.; Jiang, H.; Moult, J.; Silman, I.; Sussman, J. L. Flexibility of Aromatic Residues in the Active-Site Gorge of Acetylcholinesterase: X-ray *versus* Molecular Dynamics. *Biophysical J.* **2008**, *95*, 2500–2511.
51. Bar-On, P.; Millard, C. B.; Harel, M.; Dvir, H.; Enz, A.; Sussman, J. L.; Silman, I. Kinetic and Structural Studies on the Interaction of Cholinesterases with the Anti-Alzheimer Drug Rivastigmine. *Biochemistry* **2002,** *41*, 3555−3564.
52. Bartolucc, C.; Siotto, M.; Ghidini, E.; Amari, G.; Bolzoni, P. T.; Racchi, M.; Villetti, G.; Delcanale, M.; Lamba D. Structural Determinants of *Torpedo californica* Acetylcholinesterase Inhibition by the Novel and Orally Active Carbamate Based Anti-Alzheimer Drug Ganstigmine (CHF-2819). *J. Med. Chem*. **2006,** *49*, 5051−5058.
53. Jones, G.; Willett, P.; Glen, R. C.; Leach, A. R.; Taylor, R. Development and validation of a genetic algorithm for flexible docking. *J. Mol. Biol.* **1997**, *267*, 727−748.

54. Greig, N. H.; De Micheli, E.; Holloway, H. W.; Yu, Q.-S.; Utsuki, T.; Perry, T. A.; Brossi, A.; Ingram, D. K.; Deutsch, J.; Lahiri, D. K.; Soncrant, T. T. The Experimental Alzheimer Drug Phenserine: Pharmacodynamics and Kinetics in the Rat. *Acta Neurol. Scand.*, **2000**, *102*, 74−84.

55. Kamal, M. A.; Greig, N. H.; Alhomida, A.S.; Al-Jafari, A. A. Kinetics of Human Acetylcholinesterase Inhibition by the Novel Experimental Alzheimer Therapeutic Agent, Tolserine. *Biochem. Pharmacol.*, **2000**, *60*, 561−570.
56. (a) Brufani, M.; Filocamo, L.; Lappa, S.; Maggi, A. New Acetylcholinesterase Inhibitors. *Drugs Future*, **1997**, *22*, 397−410. (b) Imbimbo, B. P.; Martelli, P.; Troetel, W. M.; Lucchelli, F.; Lucca, U.; Thal, L. J. Efficacy and Safety of Eptastigmine for the Treatment of Patients with Alzheimer's Disease. *Neurology*, **1999**, *52*, 700−708.
57. Snape, M. F.; Misra, A.; Murray, T. K.; De Souza, R. J.; Williams, J. L.; Cross, A. J.; Green, A. R.A Comparative Study in Rats of the in vitro and in vivo Pharmacology of the Acetylcholinesterase Inhibitors Tacrine, Donepezil and NXX-066. *Neuropharmacology* **1999**, *38*, 181-93.
58. Bolognesi, M. L.; Bartolini, M.; Cavalli,A.; Andrisano, V.; Rosini, M.; Minarini,A.; Melchiorre, C.Design, Synthesis, and Biological Evaluation of Conformationally Restricted Rivastigmine Analogues. *J. Med. Chem.* **2004**, *47*, 5945−5952.
59. Trabace, L.; Cassano, T.; Steardo, L.; Pietra, C.; Villetti, G.; Kendrick, K.M.; Cuomo, V. Biochemical and Neurobehavioral Profile of CHF2819, a Novel, Orally Active Acetylcholinesterase Inhibitor for Alzheimer's Disease. *J. Pharmacol. Exp. Ther.*, **2000**, *294*, 187−194.
60. Smith, C. P.; Bores, G. M.; Petko, W.; Li, M.; Selk, D. E.; Rush D. K.; Camacho, F.; Winslow, J. T.; Fishkin, R.; Cunningham, D. M.; Brooks, K. M.; Roehr, J.; Hartman, H. B.; Davis, L.; Vargas, H. M. Pharmacological Activity and Safety Profile of P10358, A Novel, Orally Active Acetylcholinesterase Inhibitor for Alzheimer's Disease. *J. Pharmacol. Exp. Ther.*, **1997**, *280*, 710−720.
61. Mustazza, C.; Borioni, A.; Giudice, M. R. D.; Gatta, F.; Ferretti, R.; Meneguz, A.; Volpe, M. T.; Lorenzini, P. Synthesis and Cholinesterase Activity of Phenylcarbamates Related to Rivastigmine, A Therapeutic Agent for Alzheimer's Disease. *Eu. J. Med. Chem.* **2002**, *37*, 91−96.
62. (a) Decker, M. Acetylcholinesterase inhibitors based on carbamic acid quinolin-6-yl esters. *Expert Opin. Ther. Patents* **2007**, 17, 733-736. (b) Shakya, N.; Fatima, Z.; Nath, C.; Saxena, A. K. Substituted Carbamic Acid Quinolin-6-yl Esters Useful as Acetylcholinesterase Inhibitors. U. S. Patent 0142335, June 2006. (c) Marsais, F; Bohn, P.; Fur, N. L.; Levacher, V. Heterocyclic Compounds, their Preparation and their Use as Medicaments, in Particular as Anti-Alzheimer agents. U.S. Patent 062279, Mar 2009.
63. CombiGlide, version 2.5, Schrödinger, LLC, New York, NY, 2009.
64. Schrödinger Software, version 8.0; Schrödinger, LLC: New York, 2005.
65. Ellman, G. L.; Courtney, K. D.; Andres, V., Jr.; Feather-Stone, R. M. A New and Rapid Colorimetric Determination of Acetylcholinesterase Activity. *Biochem. Pharmacol.* **1961**, *7*, 88−95.
66. Brioni, J. D.; Hock, F. J.; McGaugh, J. J. Drug Effects on Learning and Memory. In, *Drug Discovery and Evaluation: Pharmacological Assays* (Vogel, G. H.; Vogel, W. H. eds.), Springer Verlag Press, New York, **1997,** pp. 335−336.
67. Das, A.; Shankar, G.; Nath, C.; Pal, R.; Singh, S.; Singh, H. K. A Comparative Study in Rodents of Standardized Extracts of *Bacopa Monniera* and *Ginkgo Biloba*: Anticholinesterase and Cognitive Enhancing Activities. *Pharmacol. Biochem. Behav.* **2002**; *73*, 893−900.
68. Todeschini R, Consonni, V. DRAGON software (version 1.11) by Milano, Italy, 2001.
69. Accelrys. Discovery Studio, version 2.0; Accelrys Inc.: San Diego, CA, 2007.

70. Yu, Q.-S.; Pei, X.-F.; Holloway, H. W.; Greig, N. H. Total Syntheses and Anticholinesterase Activities of (3aS)-N(8)-Norphysostigmine, (3aS)-N(8)-Norphenserine, Their Antipodal Isomers, and Other N(8)-Substituted Analogues. *J. Med. Chem.* **1997**, *40*, 2895−2901.
71. Yu, Q.-S.; Greig, N. H.; Holloway, H. W. Syntheses and Anticholinesterase Activities of (3aS)-N^1, N^8-Bisnorphenserine, (3aS)-N^1, N^8-Bisnorphysostigmine, Their Antipodal Isomers, and Other Potential Metabolites of Phenserine. *J. Med. Chem.* **1998**, *41*, 2371−2379.
72. Yu, Q.-S.; Holloway, H. W.; Utsuki, T.; Brossi, A.; Greig, N. H. Synthesis of Novel Phenserine-Based-Selective Inhibitors of Butyrylcholinesterase for Alzheimer's Disease. *J. Med. Chem.* **1999**, *42*, 1855−1861.
73. Yu, Q.-S.; Holloway, H. W.; Utsuki, T.; Brossi, A.; Greig, N. H. Methyl Analogues of the Experimental Alzheimer Drug Phenserine: Synthesis and Structure-Activity Relationships for Acetyl- and Butyrylcholinesterase Inhibitory Action. *J. Med. Chem.* **2001**, *44*, 4062−4071.
74. Luo, W.; Yu, Q.-S.; Zhan, M.; Parrish, D.; Deschamps, J. R.; Kulkarni, S. S.; Holloway, H. W.; Alley, G. M.; Lahiri, D. K.; Brossi, A.; Greig, N. H. Novel Anticholinesterases Based on the Molecular Skeletons of Furobenzofuran and Methanobenzodioxepine. *J. Med. Chem.* **2005**, *48*, 986−994.
75. Li, H.; Sutter, J.; Hoffman, R. HypoGen: An Automated System for Generating 3D Predictive Pharmacophore Models. In *Pharmacophore Perception, Development, and Use in Drug Design*; Guner, O. F., Ed.; International University Line: La Jolla, CA, 2000; pp 171−189.
76. Prathipati, P.; Saxena, A. K. Characterization of β_3-Adrenergic Receptor: Determination of Pharmacophore and 3D QSAR Model for β_3-Adrenergic Receptor Agonism. *J. Comput. Aided Mol. Des.* **2005**, *19*, 93−110.
77. Sprague, P. W. Automated Chemical Hypothesis Generation and Database Searching with Catalyst. In Perspectives in Drug Discovery and Design; Müller, K., Ed.; ESCOM Science Publishers B. V.: Leiden, The Netherlands, 1995; pp 1–21.
78. Brooks, B. R.; Bruccoleri, R. E.; Olafson, B. D.; States, D. J.; Swaminathan, S.; Karplus, M. CHARMm: A Program for Macromolecular Energy, Minimization, and Dynamics Calculations. *J. Comput. Chem.* **1983**, *4*, 187–217
79. Sutter, J.; Güner, O. F.; Hoffman, R.; Li, H.; Waldman, M. Effect of Variable Weight and Tolerances on Predictive Model Generation. In Pharmacophore Perception, Development, and Use in Drug Design; Güner, O. F., Ed.; International University Line: La Jolla, CA, **1999**; pp 501–511.
80. Brenner S. The genetics of *Caenorhabditis elegans*. *Genetics* **1974**, 77, 71–94.
81. Stiernagle T. Maintenance of *C. elegans* In: Hope I. *C. elegans*: A Practical Approach. Oxford University Press **1999**, 51–67.